Black hole singularity from OPE

Published for SISSA by Springer

Received: July 8, 2024
Revised: September 12, 2024
Accepted: September 28, 2024
Published: October 11, 2024

Black hole singularity from OPE

Nejc Čeplak,[a] **Hong Liu**,[b] **Andrei Parnachev**[a] **and Samuel Valach**[a]

[a]*School of Mathematics and Hamilton Mathematics Institute, Trinity College, Dublin 2, Ireland*
[b]*Center for Theoretical Physics, Massachusetts Institute of Technology, Cambridge, MA 02139, U.S.A.*

E-mail: ceplakn@tcd.ie, hong_liu@mit.edu, parnachev@maths.tcd.ie, valachs@tcd.ie

Abstract: Eternal asymptotically AdS black holes are dual to thermofield double states in the boundary CFT. It has long been known that black hole singularities have certain signatures in boundary thermal two-point functions related to null geodesics bouncing off the singularities (bouncing geodesics). In this paper we shed light on the manifestations of black hole singularities in the dual CFT. We decompose the boundary CFT correlator of scalar operators using the Operator Product Expansion (OPE) and focus on the contributions from the identity, the stress tensor, and its products. We show that this part of the correlator develops singularities precisely at the points that are connected by bulk bouncing geodesics. Black hole singularities are thus encoded in the analytic behavior of the boundary correlators determined by multiple stress tensor exchanges. Furthermore, we show that in the limit where the conformal dimension of the operators is large, the sum of multi-stress-tensor contributions develops a branch point singularity as predicted by the geodesic analysis. We also argue that the appearance of complexified geodesics, which play an important role in computing the full correlator, is related to the contributions of the double-trace operators in the boundary CFT.

Keywords: AdS-CFT Correspondence, Spacetime Singularities, Thermal Field Theory

ArXiv ePrint: 2404.17286

https://doi.org/10.1007/JHEP10(2024)105

Contents

JHEP10(2024)105

1 Introduction and summary

The AdS/CFT duality [1–3] provides a powerful laboratory for understanding quantum gravity in the bulk and conformal field theory (CFT) on the boundary. In particular, it relates black holes in AdS_{d+1} to the boundary CFT_d at finite temperature [4, 5]. CFT observables can hence be used to probe the interior of black holes and possibly the black hole singularity, see e.g. [6–22].

In [8, 9], for $d \geq 3$, signatures of black hole singularities were identified in the boundary thermal two-point functions[1]

$$G(t) = \left\langle \phi(t, \vec{0})\phi(0, \vec{0}) \right\rangle_\beta \tag{1.1}$$

where ϕ is a scalar CFT operator of conformal dimension Δ and β is the inverse temperature. In the limit of large Δ, $G(t)$ can be computed using bulk geodesics connecting the two boundary points where the operators are inserted. In [8] it was found that a specific analytically continued $G(t)$, which we denote as $\hat{G}(t)$, exhibits singularities of the form

$$\hat{G}(t) \propto \frac{1}{(t - t_c^\pm)^{2\Delta}}, \quad t \to t_c^\pm = \pm \frac{\beta e^{\mp \frac{i\pi}{d}}}{2 \sin \frac{\pi}{d}} \equiv \pm \frac{\tilde{\beta}}{2} - i\frac{\beta}{2}, \quad \Delta \to \infty \,. \tag{1.2}$$

On the gravity side, considering complex time of the form $t = t_L - i\beta/2$, with $t_L \in \mathbb{R}$, corresponds to analysing geodesics in the two-sided eternal AdS-Schwarzschild black hole. The behavior (1.2) arises because the spacelike geodesics which connect the two asymptotic regions of the black hole, approach a null geodesic bouncing off the future (past) black hole singularity as $t \to t_c^+$ ($t \to t_c^-$), see right of figure 2. We will refer to the singular behavior (1.2) as the *bouncing singularities*.

The correlator $G(t)$ can only have singularities at $t = 0$ and $t = -i\beta$. To obtain $\hat{G}(t)$, which exhibits bouncing singularities, one observes [8] that[2]

$$\mathcal{L}(t) = -\lim_{\Delta \to \infty} \frac{1}{\Delta} \log G(t), \tag{1.3}$$

develops a branch point singularity at $t = -i\frac{\beta}{2}$. Analytically continuing $\mathcal{L}(t)$ through a branch cut emanating from this branch point to the second sheet gives $\hat{\mathcal{L}}(t)$. The latter is given by the proper length of the bouncing geodesic and can be used to define

$$\hat{G}(t) \equiv e^{-\Delta \hat{\mathcal{L}}(t)} \,, \tag{1.4}$$

[1] For simplicity, the spatial separation of the operators has been set to zero.

[2] To be more precise, $\mathcal{L}(t)$ is obtained by an analytic continuation from the analogous expression using the Euclidean correlator $G(\tau)$, with $t = i\tau$. This analytic continuation is subtle and as a consequence the limit in (1.3) is not always well defined.

JHEP10(2024)105

which exhibits (1.2). In contrast, for $t = t_L - i\beta/2$, $G(t)$ is given by a sum of two complex geodesics which are regular for all t_L.

In [9] it was found that the same bouncing geodesics have direct signatures in the Fourier transform $G(\omega)$ of (1.1),[3] albeit for large imaginary frequencies,

$$G(\omega) \propto \omega^{2\Delta} e^{i t_c^{\pm} \omega}, \quad \omega \to \pm i\infty, \quad \Delta \to \infty \ . \tag{1.5}$$

The results (1.2) and (1.5) raised a number of questions whose boundary understanding has been elusive:

1. What is the CFT origin of the singular behavior in (1.2)?
2. What is CFT origin of the branch point singularity of $\mathcal{L}(t)$ at $t = -i\beta/2$ in the large Δ limit?
3. What is the boundary interpretation of the pair of complex geodesics which dominate the correlator at $t = t_L - i\beta/2$ in the large Δ limit?
4. What is the CFT origin of (1.5)?
5. The behavior (1.2) and (1.5) applies only to $d \geq 3$, as for $d = 2$ (the BTZ black hole) the black hole singularities are orbifold singularities rather than curvature singularities. What is the boundary origin of this difference?

In this paper we address these questions by investigating the behavior of thermal correlators of scalar operators by performing the Operator Product Expansion (OPE) in the boundary theory. We will restrict our discussion to the boundary theory on flat space.

The OPE of two operators ϕ separated in Euclidean time $\tau = it$ can be written schematically as

$$\phi(\tau, 0)\phi(0, 0) = \sum_n C_n \tau^{\Delta_n - 2\Delta} O_n(0), \tag{1.6}$$

where n collectively labels all operators O_n with Δ_n being their conformal dimension. The Euclidean analytic continuation of $G(t)$ can be written in terms of OPE as

$$G(\tau) \equiv G(t = -i\tau) = \frac{1}{\tau^{2\Delta}} \sum_n C_n v_n \left(\frac{\tau}{\beta}\right)^{\Delta_n}, \quad \langle O_n \rangle_\beta = v_n \beta^{-\Delta_n} \ . \tag{1.7}$$

Note that the sums in (1.6), (1.7) may have operators of the same conformal dimension which only differ by their spin. In this case, each such operator contributes a separate term in (1.6) and (1.7).

In holographic theories that are dual to Einstein gravity in the bulk,[4] the correlator (1.7) has a particularly simple structure

$$G(\tau) = G_T(\tau) + G_{[\phi\phi]}(\tau) \, . \tag{1.8}$$

[3] For notational simplicity, we use the same notation $G(\omega)$ for the Fourier transform of $G(t)$, distinguishing them only by the arguments. Similarly, below we will use the same notation $G(\tau)$ for the Euclidean analytic continuation of $G(t)$.

[4] For example, in the case of $\mathcal{N} = 4$ Super Yang-Mills theory in $d = 4$, this is the theory at large N and strong coupling.

JHEP10(2024)105

$G_T(\tau)$ is the contribution from OPEs involving multiple stress tensors, i.e. operators of the schematic form $(T_{\mu\nu})^n$, with $T_{\mu\nu}$ denoting the stress tensor, while $G_{[\phi\phi]}(\tau)$ is the contribution from double-trace operators formed from ϕ, i.e. operators of the schematic form $\phi(\partial^2)^n\partial_{i_1}\cdots\partial_{i_l}\phi$. $G_T(\tau)$ will be referred to as the stress-tensor sector of the correlator [23]. It will also be convenient to define

$$\mathcal{L}_T(\tau) = -\lim_{\Delta\to\infty}\frac{1}{\Delta}\log G_T(\tau) \tag{1.9}$$

and similarly $\mathcal{L}_{[\phi\phi]}(\tau)$.

In [24] a scheme for computing the OPE coefficients of multi-stress tensors for holographic theories in even spacetime dimensions has been presented, which enables us to compute $G_T(\tau)$ explicitly as a series expansion in τ.[5] The scheme is based on an ansatz that solves the bulk equations of motion order by order in the near-boundary expansion. The resulting OPE coefficients agree, for example, with the ones determined by bootstrap and related techniques [23, 29–32], as well as with those obtained by solving the Fourier transformed equation order by order in the OPE [21, 33–35].[6] Other nontrivial checks include comparison with the Regge limit holographic data [38–41] and geodesics in asymptotically AdS spacetimes [16, 42].

By studying the OPE data of n-stress tensor exchanges in the regime of large n, we are able to resum the full stress-tensor sector for finite Δ and show that $G_T(\tau)$ contains a singularity precisely of the form (1.2),[7]

$$G_T(\tau) \propto \frac{1}{(\tau-\tau_c^{\pm})^{2\Delta-\frac{d}{2}}}, \quad \tau\to\tau_c^{\pm} = \frac{\beta}{2} \pm i\frac{\tilde{\beta}}{2} = it_c\ . \tag{1.10}$$

We want to emphasise that despite the similar form to (1.2), this singular behaviour is obtained in the opposite limit, by first fixing Δ at a finite value and then finding the divergent behaviour of the stress-tensor sector near the singularity. The result (1.10), combined with general structure of the double-trace contribution $G_{[\phi\phi]}(\tau)$, as well as the geodesic analysis, gives a boundary picture that sheds light on various questions mentioned earlier. Here we highlight the main elements:

1. Black hole singularities are encoded in the analytic structure of the stress tensor sector of thermal correlation functions. In particular, the bouncing singularity is present at finite Δ and can be accessed by analytically continuing the stress tensor sector contribution $G_T(\tau)$ to complex values of τ without the need of going to a different sheet, which is needed to obtain $\hat{\mathcal{L}}(t)$.

   Heuristically, we may interpret the black hole geometry as being obtained from the empty AdS by "condensing" multiple gravitons, which are roughly dual to multiple stress tensors on the boundary. It thus makes intuitive sense that the black hole singularities reflect the analytic behavior of the stress tensor sector. The stress-tensor sector of thermal correlators thus possesses a large degree of universality and can serve as a direct probe of the black hole structure.

[5] See [25–28] for generalisations to other bulk theories as well as to external operators with spin.
[6] See e.g. [36, 37] for additional examples of the OPE analysis of finite temperature holographic correlators.
[7] Since (1.2) only applies to the large Δ limit, the exponents are also consistent.

JHEP10(2024)105

2. We expect that the OPE of $G(\tau)$ is uniformly convergent for all Δ only for $|\tau| < \beta/2$. This is the regime where we can take the $\Delta \to \infty$ limit inside the OPE and in doing so neglect the contributions of double-trace operators. This is why for $|\tau| < \beta/2$ the stress-tensor sector OPE fully reproduces the geodesic length [24]. At leading order in the large Δ limit,

$$\lim_{\Delta\to\infty} G(\tau) = \lim_{\Delta\to\infty} \begin{cases} G_T(\tau) & \tau < \frac{\beta}{2}\,, \\ G_{[\phi\phi]}(\tau) & \tau > \frac{\beta}{2}\,, \\ G_T(\tau) + G_{[\phi\phi]}(\tau) & \tau = \frac{\beta}{2} + it_L,\ t_L \in \mathbb{R}\,. \end{cases} \tag{1.11}$$

The branch point singularity observed in $\mathcal{L}(t)$ at $t = -\frac{i\beta}{2}$ in the geodesic analysis can be understood from the large Δ limit of $G(\tau)$. The appearance of new geodesic saddles at this point is the consequence of the "sudden" turn-on of the double trace contribution. In particular, the two terms in the last line of (1.11) can be identified respectively with the contributions of the two complex geodesics in the gravity analysis.

In addition, for $\tau > \beta/2$, the double-trace contribution ensures that the full correlator satisfies the KMS condition [43, 44]. As such, double traces are inherently linked with the periodicity in the temporal circle.

Finally, the full thermal correlator cannot contain singularities of the type (1.10). As such, the double-trace sector must also contain a singularity at the same values as the stress-tensor sector, but with opposite sign, so that the full correlator is regular.

3. We observe numerically that as Δ is increased from a finite value to infinity, $\mathcal{L}_T(\tau)$ computed using the OPE transitions between a function which is regular at $\tau = \beta/2$ and has a singularity at (1.10) and a function whose radius of convergence is $\beta/2$, where it develops a branch cut.

4. For $d = 2$, $G(\tau)$ is known exactly from conformal symmetry, and equals the corresponding Virasoro vacuum block of the heavy-heavy-light-light correlator [45]. All contributions come from the Virasoro descendants of the identity, which are the multi-stress operators,[8] with no double-trace contributions for any τ

$$G(\tau) = G_T(\tau), \quad d = 2\,. \tag{1.12}$$

Since $G(\tau)$ cannot have the bouncing singularities (1.10), neither can $G_T(\tau)$. This is related to the corresponding bulk geometry being regular.

When the CFT is put on a circle, the double-trace contributions are needed for thermal correlators to be periodic on the spatial circle. On the other hand, the corresponding bulk BTZ geometry develops an orbifold singularity. This suggests that the appearance of the black hole orbifold singularity is intrinsically linked with non-trivial double-trace contributions. This is in stark contrast with the situation in $d \geq 3$, where the analytic behavior of multiple stress-tensor exchanges appears to reflect bulk curvature singularities.

[8] We discuss this in detail in appendix D.

JHEP10(2024)105

5. The behavior (1.10) does not directly say anything regarding the momentum space behavior (1.5). It is known that (1.5) does survive to finite Δ [46]. It is thus tempting to speculate a relation

$$G(i\omega_E) \sim \int_{-\infty}^{\infty} d\tau\, e^{i\omega_E \tau} G_T(\tau), \quad \omega_E \to \pm\infty, \tag{1.13}$$

although with current available information, it is not possible to be more precise.

In section 4.4 we show that (1.11) also applies in the generalized free field (GFF) case where the thermal correlator is given by the sum over thermal images of the vacuum correlator,

$$G(\tau)^{(GFF)} = \langle \phi(\tau)\phi(0)\rangle_\beta^{(GFF)} = \sum_{m\in\mathbb{Z}} \frac{1}{(\tau + m\,\beta)^{2\Delta}}\,, \tag{1.14}$$

The sum over images ensures that the correlator satisfies the KMS condition [43, 44], $G(\tau) = G(\beta-\tau)$. Note that in (1.14) the $m = 0$ term is the contribution of the identity, while all other terms correspond to multi-trace contributions [47, 48].[9] However, there are also differences — unlike in the holographic case, $\mathcal{L}(\tau)^{(GFF)}$ does not develop a branch point at $\tau = \beta/2$.

The fact that double-trace operators do not contribute to holographic correlators for $\tau < \beta/2$ in the large-Δ limit was discussed in [24] (see also [16]). Another situation where the boundary correlator only receives contributions from the stress-tensor sector appeared in [42], where a particular near-lightcone limit was considered. In this limit, the correlators receive contributions only from the leading twist multi-stress tensor operators and can be related to spacelike one-sided geodesics.

The rest of this paper is organised as follows. In section 2 we review the relation between spacelike geodesics in eternal Schwarzschild-AdS black holes and thermal correlation functions. For definiteness, we focus on $d = 4$. In particular, we analyse the singularity associated with the bouncing geodesic. In section 3 we then analyse the OPE coefficients associated with n-stress-tensor exchanges in $d = 4$. By analysing the large-n behavior, we find (1.10). In section 4, we use the OPE analysis of section 3 to give a boundary interpretation of the results of section 2. In particular, we argue that the bouncing singularities originate from the singular behaviour found at finite Δ in the OPE analysis of the stress-tensor sector. We discuss the results in other dimensions and the generalization to the boundary CFT on a sphere, possible resolutions of the black hole singularities from α' and G_N corrections, and various future perspectives in section 5.

Some more technical details are presented in the appendices. In appendix A we discuss the general structure of thermal two-point functions. In appendix B we state the partial differential equation that we solve to determine the holographic OPE data, while in appendix C we discuss the validity of approximating the OPE series expansion by an integral. We also present some additional arguments to support the main claims of this paper. The analysis of the thermal correlator in two-dimensions is performed in detail in appendix D. In appendix E and appendix F we analyse the subleading terms in the correlator near the bouncing singularity. In the main part of the paper, we focus only on the $d = 4$ case, but we show in appendix G

[9] See also [49–51] for related earlier developments and [21, 52] for examples of recent work on manifestations of KMS conditions in CFT.

JHEP10(2024)105

that the stress-tensor sector has a singularity at the complexified time t_c which corresponds to the bouncing geodesic in other dimensions as well (we explicitly checked $d = 6$ and $d = 8$). Finally, in appendix H we discuss in detail the lowest-twist contributions to the OPE.

2 Black hole singularity from geodesics

The main object of interest in this paper are thermal two-point correlation functions of identical operators

$$G(t, \vec{x}) = \left\langle \phi(t, \vec{x}) \phi(0, \vec{0}) \right\rangle_\beta , \tag{2.1}$$

where $\beta = T^{-1}$ denotes the inverse temperature. In field theories with holographic duals these correlators can be calculated using the Green's function of the scalar field propagating in the asymptotically Anti-de Sitter black hole. When the mass, m, associated with the bulk scalar field, or equivalently, the conformal dimension of the dual field theory operator, Δ, is large, then the correlation function can be approximated by summing over classical saddles of the relevant path integral [6]

$$G(t, \vec{x}) \sim \sum_{\text{saddles}} e^{-\Delta L} . \tag{2.2}$$

These saddles correspond to the geodesics in the black-hole background that connect the boundary points at which the operators are inserted and L denotes the regularised proper length of the geodesic.

We will focus on the case where the bulk spacetime is a black brane in five dimensions[10] with the metric

$$ds^2 \;=\; -r^2 f(r)\, dt^2 + \frac{dr^2}{r^2 f(r)} + r^2 d\vec{x}^2 , \tag{2.3}$$

where $\vec{x} = (x, y, z)$, so that $d\vec{x}^2$ denotes the flat metric on $\mathbb{R}^3$, and

$$f(r) \equiv 1 - \frac{\mu}{r^4} . \tag{2.4}$$

Note that in most of this paper we set the radius of AdS to unity. Near the spacetime boundary, $r \to \infty$, the metric (2.3) reduces to that of the Poincaré patch of AdS_5. As such, the conformal boundary is just four-dimensional Minkowski space $\mathbb{R}^{1,3}$. The parameter μ is related to the inverse temperature β through $\mu = (\pi/\beta)^4$. For the remainder of this section, we set $\mu = 1$, which means that $\beta = T^{-1} = \pi$ and the location of the black-hole horizon is given by $r_0 = 1$. The curvature singularity is at $r = 0$.

We are interested in the maximally extended spacetime which can be described by using complexified Schwarzschild coordinates. The time coordinate t then has a real and imaginary part, which we denote as[11]

$$t = t_{\rm L} - i\, t_{\rm E} , \qquad t_{\rm L} \in \mathbb{R} , \quad 0 \le t_{\rm E} < \beta . \tag{2.5}$$

The Lorentzian section of this spacetime can be divided into four wedges in which the imaginary part takes different constant values, summarised in figure 1. Regions I and III

[10] Examples in higher dimensions are discussed in appendix G.

[11] Note that we use a different sign convention for the imaginary part compared to [8, 9].

JHEP10(2024)105

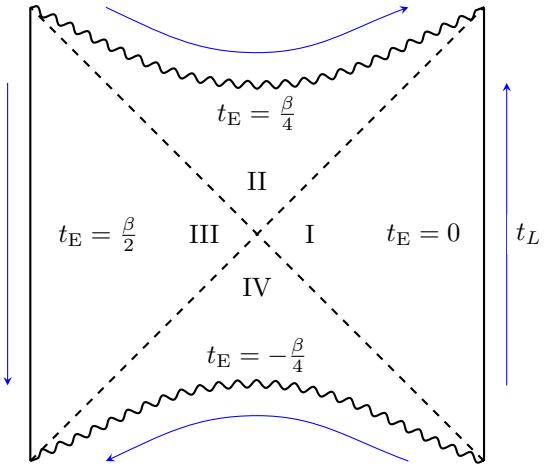

Figure 1. The Penrose diagram for the Lorentzian section of the maximally extended black-hole geometry in AdS_5. The spacetime separates into four regions with different constant values for the imaginary part of the time-coordinate. The blue arrows depict the direction of Lorentzian time, t_L, in each region.

describe two spacelike separated regions outside the horizons. We choose the imaginary part of the time coordinate in Regions I and III to be given by $t_{\rm E} = 0$ and $t_{\rm E} = \beta/2$ respectively. Region II describes the interior of the black hole with $t_{\rm E} = \beta/4$, while Region IV is the white hole region, where $t_{\rm E} = -\beta/4$. In essence, crossing a horizon corresponds to shifting the imaginary part of the time coordinate by $\beta/4$.

In what follows we review the analysis of the geodesic approximation to the correlator $G(t_L - i\beta/2, \vec{x})$, which can be interpreted as a two-sided correlator with the operators in (2.1) being inserted at different asymptotic regions of the complexified spacetime (2.3). As shown in [8, 9], real spacelike geodesics that connect the two asymptotic regions probe the interior of the black hole, see figure 2. As they probe deeper into the interior, the geodesics become more and more light-like with their proper length vanishing. This singular behavior is incompatible with the general properties of thermal correlation functions, which shows that such "bouncing geodesics" cannot contribute to the path integral. However, in the next section we show that the diverging behaviour related to the bouncing geodesics is still encoded in the stress-tensor sector of the OPE.

2.1 Geodesics in the Euclidean section

We begin by analysing geodesics in the Euclidean section of the black-brane spacetime

$$ds^2 \;=\; r^2\, f(r)\, d\tau^2 \;+\; \frac{dr^2}{r^2\, f(r)} \;+\; r^2\, d\vec{x}^2\,, x \tag{2.6}$$

where $f(r)$ is defined in (2.4) and $\tau \sim \tau + \beta$ is periodically identified.[12] We can use the symmetries of the metric to reduce the problem to the motion in a one-dimensional effective

[12]The coordinate τ is related to the usual time coordinate through Wick rotation, $\tau = i\,t = t_{\rm E} + i\,t_{\rm L}$, which explains our choice of sign for the imaginary part in (2.5). In this subsection, we take $\tau \in \mathbb{R}$, while we will extend it to full complex space in subsequent sections.

JHEP10(2024)105

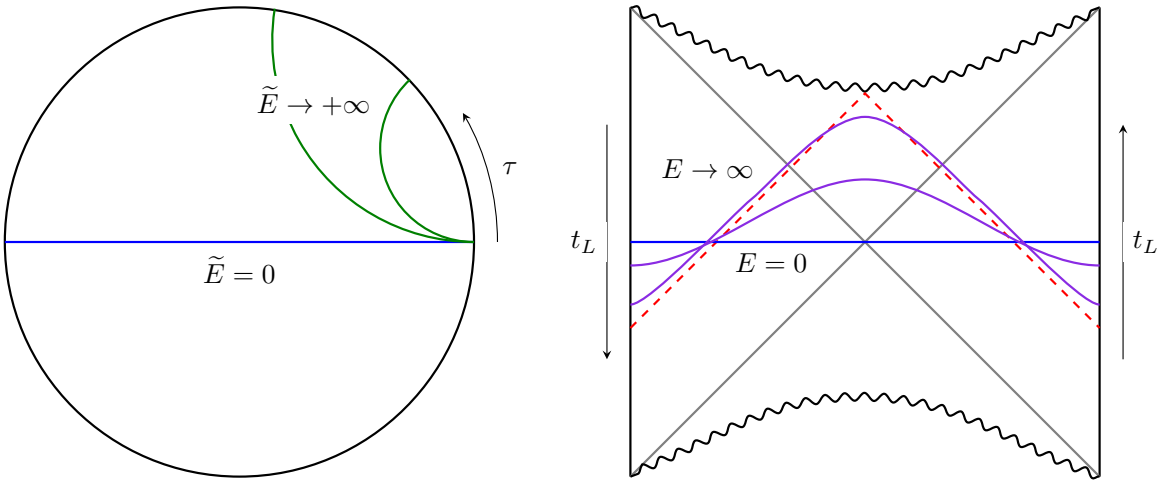

Figure 2. Diagrams for the Euclidean section (left) and the Lorentzian section (right) of the complexified black-hole spacetime. In both, we plot spacelike geodesics: the $\widetilde{E} = E = 0$ geodesic (blue) can be drawn in both sections. On the left, the green curves depict geodesics with increasing $\widetilde{E}$, which correspond to taking the limit $\tau \to 0$. On the right, in purple, we plot real geodesics that probe the black-hole interior. As $E = -i\widetilde{E} \to \infty$, the geodesics become light-like signalling singular behaviour — these are the Bouncing geodesics [8, 9].

potential. In general, we can introduce the energy, $\widetilde{E}$, associated with the time-translation invariance, and linear momenta P_i, related to the $\mathbb{R}^3$ isometry. In the main text we limit ourselves to the case with $x = 0$, so that all linear momenta are set to zero.[13]

Let the geodesic be parameterised by an affine parameter s and denote the derivative with respect to this parameter with a dot, for example $\dot{\tau}(s)$. The energy of a geodesic is given by

$$\widetilde{E} = r^2 f(r) \dot{\tau} \,, \tag{2.7}$$

defined in such a way that $\dot{\tau} > 0$ for $\widetilde{E} > 0$. The condition that the geodesic is everywhere spacelike can be rearranged into

$$\dot{r}^2 = r^2 f(r) - \widetilde{E}^2 \,. \tag{2.8}$$

Geodesics in the Euclidean section are pictured on the left of figure 2. They start at $r = \infty$ and probe the space up to a minimal value, r_t, which we call the turning point, before returning to the asymptotic boundary. The turning point is given by the largest real root at which (2.8) vanishes

$$r_t^2 = \frac{1}{2}\left(\widetilde{E}^2 + \sqrt{\widetilde{E}^4 + 4}\right) \,. \tag{2.9}$$

[13]The case with non-vanishing spatial separation is considered in appendix F.

JHEP10(2024)105

The time difference between the endpoints of a geodesic is given by

$$\begin{aligned}\tau \equiv \tau_f - \tau_i &= 2\int_{r_t}^{\infty} \frac{\widetilde{E}\, dr}{r^2\, f(r)\sqrt{r^2\, f(r) - \widetilde{E}^2}} \\ &= \frac{1}{2}\log\left(\frac{\widetilde{E}^2 + 2\,\widetilde{E} + 2}{\sqrt{\widetilde{E}^4 + 4}}\right) - \frac{i}{2}\log\left(\frac{\widetilde{E}^2 + 2\,i\,\widetilde{E} - 2}{\sqrt{\widetilde{E}^4 + 4}}\right). \end{aligned} \tag{2.10}$$

Let us focus on the behaviour at high energies, $\widetilde{E} \to \infty$. In this limit, the turning point goes toward the asymptotic boundary — such geodesics probe only the asymptotic region of space. To see how the time difference scales with the energy, we expand (2.10)

$$\tau = \frac{2}{\widetilde{E}} - \frac{8}{5\,\widetilde{E}^5} + \mathcal{O}\left(\widetilde{E}^{-9}\right), \quad \Longrightarrow \quad \widetilde{E} = \frac{2}{\tau} - \frac{\tau^3}{10} + \mathcal{O}\left(\tau^7\right), \tag{2.11}$$

meaning that as the energy is increased, the time difference goes to 0.

The regularised proper length of the geodesic is given by

$$L = 2\lim_{r_{\max}\to\infty}\left[\int_{r_t}^{r_{\max}} \frac{dr}{\sqrt{r^2\, f(r) - \widetilde{E}^2}} - \log r_{\max}\right] = \frac{1}{2}\log\left(\frac{16}{\widetilde{E}^4 + 4}\right), \tag{2.12}$$

where $r_{\max}$ is the UV cut-off length [9]. By expressing the energy as a function of τ we find a logarithmic divergence at the origin

$$L = 2\log\tau - \frac{\pi^4}{40}\left(\frac{\tau}{\beta}\right)^4 - \frac{11\,\pi^8}{14400}\left(\frac{\tau}{\beta}\right)^8 + \mathcal{O}\left(\tau^{12}\right), \tag{2.13}$$

where we have reinstated the appropriate units, using $\beta/\pi = 1$. When $\Delta \gg 1$, the sum over geodesics gives an approximation to the thermal correlation function. And by exponentiating (2.13) we get the contribution from the spacelike geodesic connecting two points on the Euclidean time circle

$$e^{-\Delta L} = \frac{1}{\tau^{2\Delta}}\left[1 + \frac{\Delta\,\pi^4}{40}\left(\frac{\tau}{\beta}\right)^4 + \frac{(9\Delta^2 + 22\Delta)\,\pi^8}{28800}\left(\frac{\tau}{\beta}\right)^8 + \mathcal{O}\left(\tau^{12}\right)\right]. \tag{2.14}$$

In the next section we will show that this result is completely reproduced by only the stress-energy sector in the large-Δ limit.

2.2 Contributions from different saddles

The expressions (2.10) and (2.12) can be analytically continued to complex $\widetilde{E}$ to obtain geodesics in the real section of Schwarzschild spacetime. In particular, to obtain two-sided correlation functions, we need to consider

$$\tau = \frac{\pi}{2} + it_L, \quad t_L \in \mathbb{R}\,. \tag{2.15}$$

For this purpose, expanding (2.10) around $\widetilde{E} = 0_+$, we find

$$\tau - \frac{\pi}{2} = -\frac{\widetilde{E}^3}{6} + O(\widetilde{E}^5), \qquad L = \log[2] - \frac{\widetilde{E}^4}{8} + O(\widetilde{E}^8), \tag{2.16}$$

JHEP10(2024)105

which implies that $L(\tau)$ has a branch point singularity of the form $(\tau-\frac{\pi}{2})^{\frac{4}{3}}$ at $\tau=\frac{\pi}{2}$. Solving $\widetilde{E}$ in terms of τ we find three branches of solutions

$$\widetilde{E}_0=(6r)^{\frac{1}{3}}\,e^{\frac{i\theta}{3}},\quad \widetilde{E}_1=\widetilde{E}_0\,e^{-\frac{2\pi i}{3}},\quad \widetilde{E}_2=\widetilde{E}_0\,e^{-\frac{4\pi i}{3}},\quad \frac{\pi}{2}-\tau\equiv r\,e^{i\theta}\ . \tag{2.17}$$

For $\frac{\pi}{2}-\tau>0$ (i.e. $\theta=0$), $\widetilde{E}_0$ branch should be chosen. To analytically continue $L(\tau)$ to τ given by (2.15), we decrease θ from 0 to $-\frac{\pi}{2}$ (for definiteness take $t_L>0$). A careful analysis [8][14] shows that in the large Δ limit:

1. For $\theta\in(-\frac{\pi}{8},0]$, $\widetilde{E}_0$ is the only saddle contributing to $G(\tau)$.
2. For $\theta\in(-\frac{\pi}{2},-\frac{\pi}{8}]$, $\widetilde{E}_0$ is the dominant saddle, but now $\widetilde{E}_1$ also contributes as a subdominant saddle, i.e.
$$G(\tau)\sim e^{-\Delta L(\widetilde{E}_0)}+e^{-\Delta L(\widetilde{E}_1)}\ . \tag{2.18}$$
3. At $\theta=-\frac{\pi}{2}$, i.e. for two-sided geodesics, the two terms in (2.18) have the same norm and thus contribute equally. Both $\widetilde{E}_0$ and $\widetilde{E}_1$ are complex, corresponding to complex geodesics in the black hole spacetime.[15]
4. For $\theta\in[-\frac{7}{8}\pi,-\frac{\pi}{2})$, we still have (2.18), but now $\widetilde{E}_0$ contribution is subdominant.
5. For $\theta\in[-\pi,-\frac{7}{8}\pi)$ only $\widetilde{E}_1$ contributes. In particular, for $\theta=-\pi$, i.e. $\tau>\beta/2$, we have $\widetilde{E}_1$ becomes real, negative, and
$$-\frac{1}{\Delta}\log G(\tau)=L(\widetilde{E}_1(\tau))=L(\widetilde{E}_0(\beta-\tau))=-\frac{1}{\Delta}\log G(\beta-\tau),\quad \tau\in\left(\frac{\beta}{2},\beta\right)\ . \tag{2.19}$$
This shows that $G(\tau)$ in the large Δ limit satisfies the KMS condition.
6. The saddle corresponding to $\widetilde{E}_2$ does not lie on the steepest descent contour of the integral to obtain $G(\tau)$ [8, 9], and never contributes to the correlator.

2.3 Bouncing geodesics

The $\widetilde{E}_2$ branch in (2.17), which never contributes to the correlator, corresponds to the two-sided real geodesics presented in the right plot of figure 2. More explicitly, for $\theta=-\frac{\pi}{2}$ we have

$$\widetilde{E}_2=i\,E\,,\qquad E\in\mathbb{R}_+\,, \tag{2.20}$$

The turning point is then given by[16]

$$r_t^2=\frac{1}{2}\left(\sqrt{E^4+4}-E^2\right)\ . \tag{2.21}$$

[14] See section 3.4 of the paper. While the discussion in section 3.4 was phrased as a model, it can be justified using section 4.4 of [9].

[15] See [53, 54] for recent discussion of complexified geodesics in the de Sitter context.

[16] The analytic structure of the turning point as a function of the energy, $r_t(\widetilde{E})$, is discussed in [9]. This function has branch cuts in the complex plane that can be associated to quasinormal modes of the black hole. Then one can define $r_t(\widetilde{E})$ in the full complex $\widetilde{E}$ plane by starting from (2.8) for $\widetilde{E}\in\mathbb{R}$ and analytically continue through the origin. Physically this can be thought of as following the geodesics in the Euclidean section as the real part of the energy is decreased from infinity to 0. At this point the geodesic crosses the cap or equivalently traverses the double-sided Lorentzian section (see the two geodesics in blue in figure 2). One then increases the imaginary part of the energy, E, causing the geodesics to probe the region behind the horizon.

JHEP10(2024)105

One can see that the turning point is inside the horizon for $E^2 > 0$. In fact, as $E \to \infty$, the turning point approaches the origin as $r_t \sim 1/E$, meaning that in this regime the geodesics probe the region near the singularity, see right of figure 2.

The time difference and the proper length of the two-sided geodesics corresponding to $\widetilde{E}_2$ can be obtained by taking $\widetilde{E} = i\,E$ in (2.10) and (2.12)

$$\tau = \frac{\pi}{2}(1+i) + \frac{1}{2}\log\left(\frac{E^2 - 2i\,E - 2}{\sqrt{4+E^4}}\right) - \frac{i}{2}\log\left(\frac{E^2 + 2\,E + 2}{\sqrt{4+E^4}}\right), \tag{2.22a}$$

$$\hat{\mathcal{L}} \equiv L(\widetilde{E}_2) = \frac{1}{2}\log\left(\frac{16}{E^4+4}\right). \tag{2.22b}$$

which matches the known results [8, 9]. We have also identified $\hat{\mathcal{L}}$, which was introduced around (1.4), as the geodesic distance associated with $\tilde{E}_2$. We keep the constant time shift explicit — the real part corresponds to the shift of $\tau = \beta/2$ which comes from the spacelike geodesic crossing two horizons as it goes from the I to the III patch in the Lorentzian section of the spacetime.

Denote the time shift observed above as

$$\tau_c \equiv \frac{\pi}{2}(1+i) = \frac{\pi}{\sqrt{2}}\,e^{\frac{i\,\pi}{4}}, \tag{2.23}$$

and expanding (2.22a) in large E gives

$$\tau = \tau_c - \frac{2\,i}{E} + \frac{8\,i}{5\,E^5} + \mathcal{O}\left(E^{-9}\right), \tag{2.24}$$

meaning that as $E \to \infty$, and the spacelike geodesics become increasingly null-like, $\tau \to \tau_c$. Let

$$\delta\tau \equiv \tau_c - \tau\,, \tag{2.25}$$

and perturbatively invert (2.22a) to express E as a function of $\delta\tau$

$$E = \frac{2i}{\delta\tau} - \frac{i}{10}\,(\delta\tau)^3 + \mathcal{O}\left((\delta t)^7\right). \tag{2.26}$$

One can then insert this into the expression for proper length and again find a logarithmic divergence, only now as $\tau \to \tau_c$

$$\hat{\mathcal{L}} = 2\log\delta\tau + \frac{\pi^4}{160}\left(\frac{\delta\tau}{\tau_c}\right)^4 + \mathcal{O}\left(\delta\tau^8\right), \tag{2.27}$$

where we have reinstated the units using $\pi^4 = \beta^4 = -4\,\tau_c^4$. We note that the first correction to the logarithmic divergence appears at order $(\delta\tau)^4$. We then find

$$\hat{G} \equiv e^{-\Delta\,\hat{\mathcal{L}}} = \frac{1}{(\delta\tau)^{2\Delta}}\left[1 - \frac{\Delta\,\pi^4}{160}\left(\frac{\delta\tau}{\tau_c}\right)^4 + \mathcal{O}\left(\delta\tau^8\right)\right], \tag{2.28}$$

which exhibits the singular behavior (1.2).

JHEP10(2024)105

3 Black hole singularity from OPE

In this section we holographically extract the OPE coefficients of the n-stress tensor contributions to the thermal correlator. We then find the large-n behaviour of these coefficients, which allows us to resum the stress-tensor sector of the correlator near the radius of convergence of the OPE. In $d = 4$, for finite Δ we find singularities in the complex τ-plane, located at $\tau_c = \frac{\beta}{\sqrt{2}} e^{i\frac{\pi}{4}+ik\frac{\pi}{2}}$ for $k \in \mathbb{Z}$. These correspond to the singularities associated with bouncing geodesics discussed in the previous section and are direct signatures of the black hole singularity. We further show that these bouncing singularities disappear in the large Δ limit, where we recover the branch point singularity at $\tau = \beta/2$. This is consistent with the geodesic analysis performed in the previous section.

3.1 Stress-tensor sector of the correlation function

Consider the scalar two-point function at finite temperature $T = \beta^{-1}$

$$G(\tau, \vec{x}) = \langle \phi(\tau, \vec{x}) \phi(0,0) \rangle_\beta \,. \tag{3.1}$$

Let the CFT be holographically dual to a planar AdS-Schwarzschild black hole in $(d+1)$-dimensions and the scalar operators be dual to minimally coupled scalar fields in the bulk. We again use the black hole metric in the Euclidean signature (2.6)

$$ds^2 \;=\; r^2\, f(r)\, d\tau^2 \;+\; \frac{dr^2}{r^2\, f(r)} \;+\; r^2\, d\vec{x}^2 \,, \tag{3.2}$$

with $\vec{x} = (x, y, z)$, and $f(r) = 1 - \frac{\mu}{r^d}$. In this section we keep the parameter $\mu = (4\pi/d\,\beta)^d$ explicit. The equation of motion for the minimally coupled scalar

$$(\Box - m^2)\phi = 0 \,, \qquad m^2 = \Delta(\Delta - d) \tag{3.3}$$

can be solved by a near-boundary expansion [24]. We first perform a coordinate transformation $(\tau, \vec{x}, r) \;\to\; (w, \rho, r)$

$$\rho^2 = r^2\, \vec{x}^2 \,, \qquad w^2 = 1 + r^2(\tau^2 + \vec{x}^2) \,, \tag{3.4}$$

and write

$$\phi(w, \rho, r) = \left(\frac{r}{w^2}\right)^\Delta \psi(w, \rho, r) \,, \tag{3.5}$$

where $(r/w^2)^\Delta$ is the solution in the pure AdS space. The equation of motion (3.3) then reduces to a differential equation for $\psi(w, \rho, r)$, whose explicit form in arbitrary dimension d is given in appendix B. Using the standard AdS/CFT dictionary, the boundary correlator can be obtained by taking the limit

$$G(\tau, \vec{x}) = \frac{1}{(\tau^2 + \vec{x}^2)^\Delta} \lim_{r\to\infty} \psi \,. \tag{3.6}$$

Determining the function ψ using the bulk equation of motion determines the boundary correlation function.

JHEP10(2024)105

There are two types of contributions to ψ — in terms of the CFT description, one corresponds to the stress-tensor sector, while the other contains the contributions of the double-trace operators. We restrict ourselves to non-integer conformal dimensions, in which case the two sectors decouple[17]

$$\psi = \psi_T + \psi_{[\phi\phi]}\,, \tag{3.7}$$

where ψ_T denotes the stress tensor sector, which also includes the contribution dual to the identity operator, while $\psi_{[\phi\phi]}$ denotes the double-trace contributions. We focus on the stress tensor sector. Its near-boundary expansion is given by [24]

$$\psi_T = 1 + \sum_{i=1}^{\infty} \sum_{j=0}^{i} \sum_{k=-i}^{\frac{d\,i}{2}-j} a^i_{j,k} \frac{\rho^{2j} w^{2k}}{r^{d\,i}}\,, \tag{3.8}$$

where 1 corresponds to the contribution of the identity operator. By inserting this ansatz into the equation of motion of the bulk scalar and expanding to arbitrary order in $1/r$, one is able to determine the coefficients $a^i_{j,k}$. Most importantly, through the dictionary (3.6), this large-r expansion on the bulk side systematically maps to the OPE of the boundary correlator, which for $\vec{x} = 0$ reads[18]

$$G_T(\tau) = \frac{1}{\tau^{2\Delta}} \sum_{n=0}^{\infty} \Lambda_n \left(\frac{\tau}{\beta}\right)^{d\,n}\,, \tag{3.9}$$

where the subscript in $G_T(\tau)$ denotes that this is only the stress-tensor sector of the full correlator, $G(\tau)$.[19] Through this expression we are able to determine the stress-tensor contributions to Λ_n using the near-boundary expansion of ψ_T.

It is important to emphasise that using this procedure one cannot determine the full correlation function but only the stress tensor sector. Namely, double trace operators are sensitive to the near-horizon behaviour, hence their OPE data cannot be determined from the near-boundary analysis that is central to this method [24]. We also want to stress that this method utilises two expansions in large-r: in (3.8) one first uses such an expansion to solve the bulk equations of motion followed by a second $r \to \infty$ limit to obtain the correlation function (3.6). This double-r limit is crucial, but it makes the method conceptually less transparent. Nonetheless, we consider the OPE data obtained from this method to be exact to all orders in Δ. While we are currently lacking a definite proof that this is the case, the results of this method were shown to be consistent with those obtained by alternative techniques.

In what follows, we focus on the correlation functions where the operators are inserted at the same spatial points, with correlators at $\vec{x} \neq 0$ considered in appendix F.

3.2 OPE coefficients and the KMS condition

Let us now set $d = 4$. For small values of n, one can efficiently calculate the Λ_n as explicit functions of Δ. After that, calculating Λ_n for general Δ becomes too time-demanding, so

[17] For integer Δ the two sectors mix and situation becomes more subtle [24].

[18] See appendix A for more details.

[19] With an abuse of nomenclature, we will still refer to $G_T(\tau)$ as the correlator. The subscript should serve as a reminder that it is just the stress-tensor sector contribution.

JHEP10(2024)105

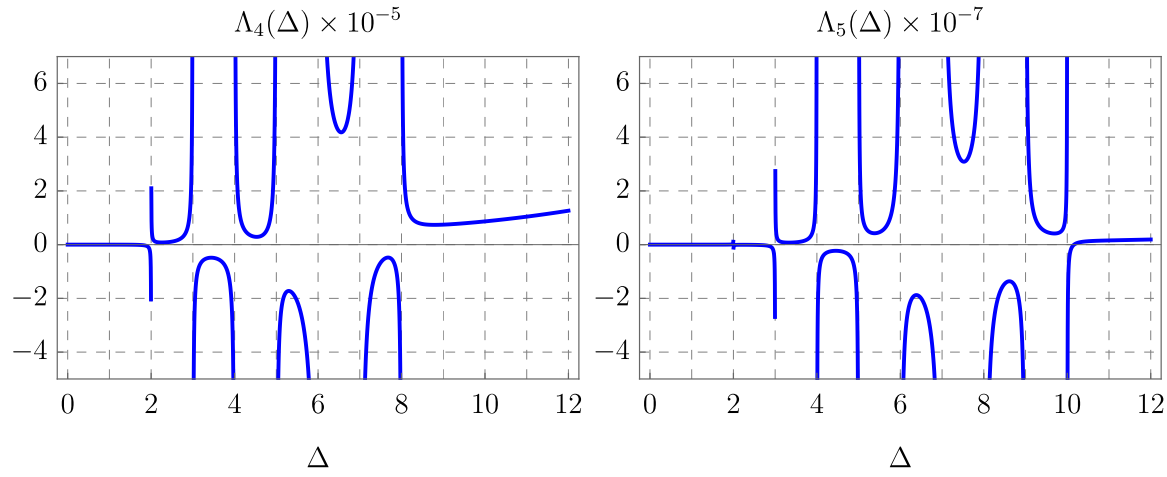

Figure 3. Plots for Λ_4 and Λ_5 as functions of Δ. These OPE coefficients have poles at $\Delta = 2, 3, \ldots, 2n$ and are regular for $\Delta > 2n$.

we first fix Δ to a certain value and only then calculate Λ_n. Namely, as n grows, these coefficients become more complicated functions of Δ. For example, the first few terms in the small τ expansion of the correlator are given by

$$G_T(\tau) \approx \frac{1}{\tau^{2\Delta}}\left[1 + \frac{\pi^4\,\Delta}{40}\left(\frac{\tau}{\beta}\right)^4 + \frac{\pi^8\,\Delta\,(63\Delta^4 - 413\Delta^3 + 672\Delta^2 - 88\Delta + 144)}{201600(\Delta-4)(\Delta-3)(\Delta-2)}\left(\frac{\tau}{\beta}\right)^8 + \ldots\right]. \tag{3.10}$$

The expressions for Λ_n with higher n follow the same pattern as Λ_2 above (see figure 3 for Λ_4 and Λ_5 as functions of Δ) and can be schematically written as

$$\Lambda_n \sim \frac{h_n(\Delta)}{\prod_{k=2}^{2n}(\Delta - k)}\,, \tag{3.11}$$

where $h_n(\Delta)$ is a polynomial function.

Fixing n and varying Δ, we can distinguish two regimes: $\Delta \leq 2n$, where we find poles at $\Delta = 2, 3, \ldots, 2n$, and $\Delta > 2n$, where the OPE coefficients have no poles in Δ. For fixed Δ, the OPE coefficients in these two regimes behave differently, which can be seen in figure 4. We see a significant change in the behaviour at a particular value $n = n_*$. Analysing the dependence of this cross-over point on the conformal dimension, we find that $n_* = \Delta/2$,[20] which is exactly where we find the last pole in Λ_n.

That the cross-over happens at this precise value of n should not be surprising. Namely, recall from (3.9) that the conformal dimension of the $(T_{\mu\nu})^n$ multi-stress tensor exchange in d dimensions is $\Delta_{T^n} = n\,d$, while those for double-trace operators have $\Delta_m = 2\Delta + 2m$, $m = 0, 1, 2, \ldots$. They can mix when $\Delta_{T^n} = \Delta_m$, which are exactly the locations of the poles of Δ in Λ_n for a fixed n, and are only possible for $n \geq n_*$ with

$$n_* \equiv \frac{2\Delta}{d} \overset{d=4}{=} \frac{\Delta}{2}\,, \quad \Longleftrightarrow \quad \Delta^*_{T^n} \equiv n_*\,d = 2\,\Delta\,. \tag{3.12}$$

[20] In practice, we have taken n_* to be the lowest integer greater than $\Delta/2$, which is why all points lie just above the $\Delta/2$ line on the right plot in figure 4.

JHEP10(2024)105

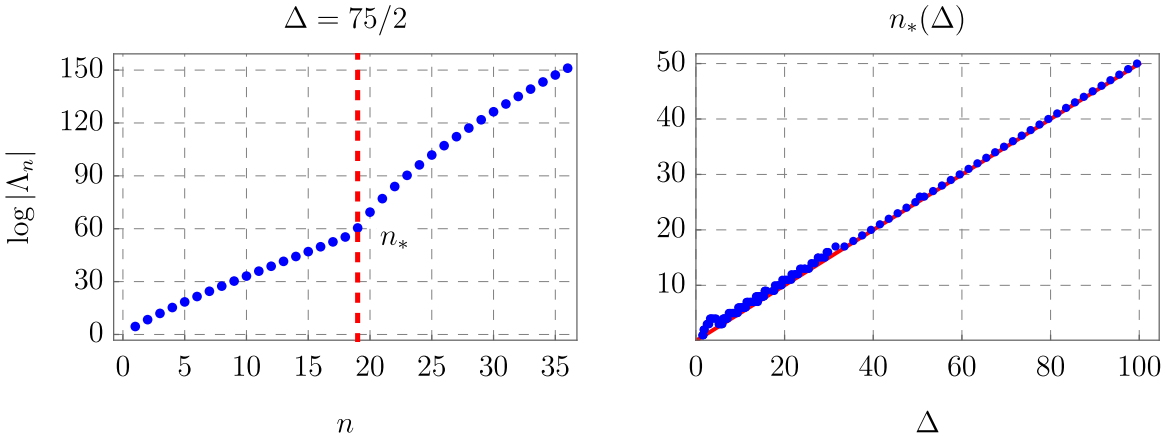

Figure 4. On the left we plot the values of $\log|\Lambda_n|$ for $\Delta = \frac{75}{2}$. We see that at $n_* = 19$, there is a change of behaviour of the OPE coefficients. On the right, we plot the behaviour of n_* as a function of Δ and find that $n_* = \Delta/2$ (red).

This explains the different behavior of Λ_n for $n > n_*$ and $n < n_*$ observed in the left plot of figure 4. We can equivalently say that the cross-over point happens exactly at the point where double-trace operators start contributing; for $n < n_*$, the series expansion for $G(\tau)$ has only contributions from $G_T(\tau)$.

In our analysis, we have no control over the double-trace contributions. Therefore, for finite Δ, $G_T(\tau)$ does not reproduce the full thermal correlation function. A simple check of the importance of the double-trace exchanges comes from the failure of the stress-tensor sector to satisfy the KMS condition. In figure 5, we plot numerically $G_T(\tau)$ for various Δ, and see that $G_T(\tau)$ is not symmetric around $\tau = \beta/2$ and thus $G_T(\tau) \neq G_T(\beta - \tau)$. The stress-tensor sector contribution by itself does not satisfy the KMS condition and contains no knowledge about the periodicity of the (Euclidean) time circle. Hence one role of the double-trace sector is to ensure that the full correlator satisfies the KMS condition.

3.3 Asymptotic analysis of OPE coefficients for finite Δ and bouncing singularities

Let us now focus on the analysis of the coefficients Λ_n for large values of n and finite Δ. We are thus interested in the regime where $n > n_*$ and both the stress-tensor and double-trace contributions are appearing in the full correlator. As already mentioned above, calculating Λ_n as explicit functions of Δ is currently out of our computational reach. Instead we first fix Δ to a finite number: for each value of Δ considered, we calculated $n \approx 50$ coefficients, which on a standard desktop computer takes around 10 days per Δ.

We find that for large values of n, the Λ_n can be approximated by (see figure 6)

$$\Lambda_n^a = c(\Delta)\, \frac{n^{2\Delta-3}}{\left(\frac{1}{\sqrt{2}}\right)^{4n} e^{i\pi n}}\,. \tag{3.13}$$

One can be more precise and include $1/n$ corrections to (3.13). We analyse such terms and how we obtained the form for Λ_n^a in detail in appendix E. The $1/n$ corrections become

JHEP10(2024)105

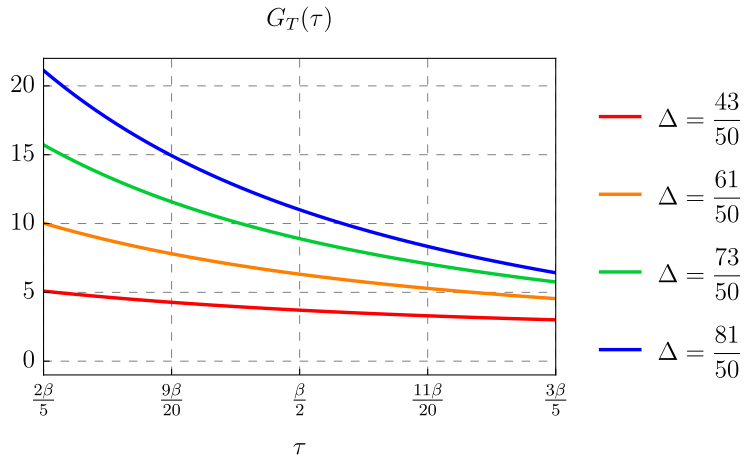

Figure 5. The value of stress-tensor contribution to the thermal correlator for different values of Δ near $\tau = \beta/2$. We see that the stress-tensor sector is not symmetric around $\tau = \beta/2$ and thus does not satisfy the KMS condition, $G_T(\tau) = G_T(\beta - \tau)$.

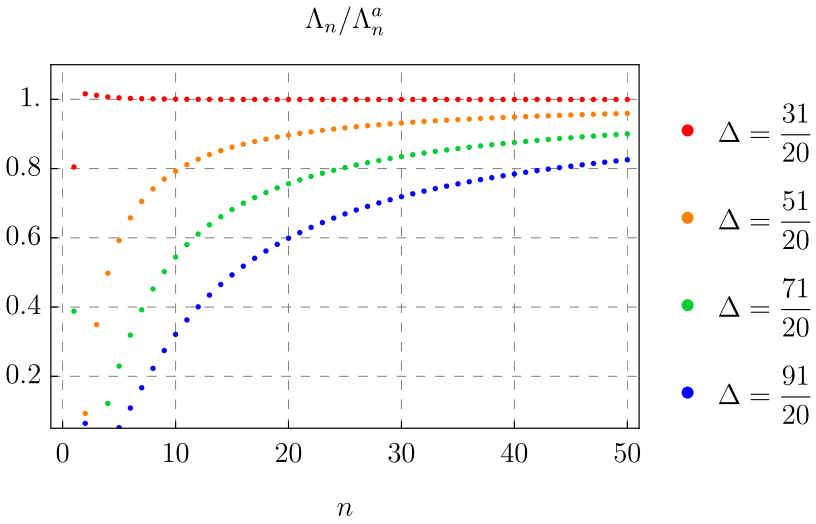

Figure 6. Ratio of the explicit results for Λ_n to the leading large-n prediction for different values of Δ in $d = 4$.

especially important at large Δ, which can already be seen in figure 6, where the approach to the asymptotic form is slower for higher Δ.

The coefficients Λ_n^a contain a non-trivial function $c(\Delta)$, which has poles at $\Delta = 2, 3, \ldots$.[21] This diverging behaviour can be isolated through

$$c(\Delta) \equiv \frac{\pi\,\Delta\,(\Delta-1)}{\sin(\pi\,\Delta)}\,\hat{c}(\Delta)\,, \qquad \text{for} \quad \Delta > 0\,, \tag{3.14}$$

[21] As mentioned earlier, at integer values of Δ the double trace operators can mix with the stress tensor sector. The addition of these double traces should cancel the divergence and make the correlation function finite [24].

JHEP10(2024)105

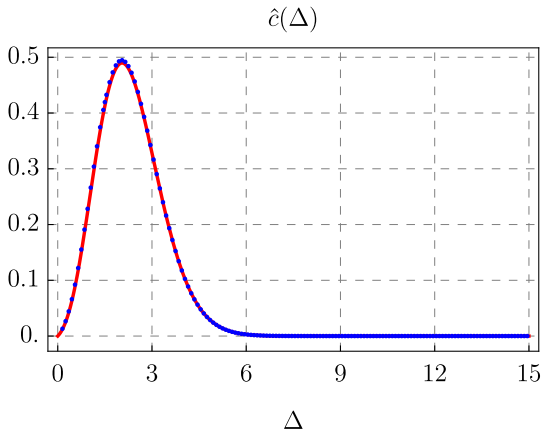

Figure 7. Numerical data for $\hat{c}(\Delta)$ (blue) compared with the function given in (3.14) (red).

where the function $\hat{c}(\Delta)$ is free of poles. It turns out (see figure 7), that this residual function can be approximated by[22]

$$\hat{c}(\Delta) \approx \frac{\Delta}{\Gamma\left(2\,\Delta+\frac{3}{2}\right)}\,\frac{4^{2\Delta}}{20}\,. \tag{3.15}$$

We now insert the asymptotic form of Λ_n into the OPE of the correlator (3.9) and approximate the sum with an integral[23]

$$G_T(\tau) \approx \frac{1}{\tau^{2\Delta}}\int_0^\infty \Lambda_n^a \left(\frac{\tau}{\beta}\right)^{4n} dn = \frac{c(\Delta)\,\Gamma(2\Delta-2)}{\tau^{2\Delta}}\left[-\log\left(\frac{\tau^4}{\left(\frac{\beta}{\sqrt{2}}\right)^4 e^{i\pi}}\right)\right]^{-(2\Delta-2)}\,. \tag{3.16}$$

While this form of the correlator is not valid for all values of τ, it gives us information about its behaviour near singular points: namely, the (3.16) will diverge whenever the argument of the logarithm is equal to 1, which is precisely at

$$\tau = \tau_c \equiv \frac{\beta}{\sqrt{2}} e^{i\frac{\pi}{4}+ik\frac{\pi}{2}} \quad \text{for} \quad k\in\mathbb{Z}\,. \tag{3.17}$$

Let $\delta\tau \equiv \tau_c - \tau$. Near the critical values, the correlator takes the form

$$G_T(\tau\approx\tau_c) \sim \frac{c(\Delta)\,\Gamma(2\Delta-2)}{4^{(2\Delta-2)}}\,\frac{1}{\tau_c^2}\,\frac{1}{\delta\tau^{2\Delta-2}}\,, \tag{3.18}$$

which is precisely of the form of the bouncing singularities (1.2) (see figure 8). The four-fold rotational symmetry of the singularities (3.17) originates from the fact that multiplying by a fourth root of unity $\tau \to e^{i\frac{k\pi}{2}}\tau$ leaves all terms inside the sum in the OPE (3.9) invariant.

At first sight, one can now take the large-Δ limit of the correlator near the poles. To make a valid comparison, we first define

$$\overline{\mathcal{L}}_T \equiv -\frac{1}{\Delta}\,\log G_T(\tau)\,, \tag{3.19}$$

[22] That is, for $\Delta \gtrsim 5/4$ and up to $\Delta \approx 15$, the ratio between the "numerical" values and (3.14) is equal to 1 up to 2%.

[23] We discuss the validity of this approximation in appendix C.

JHEP10(2024)105

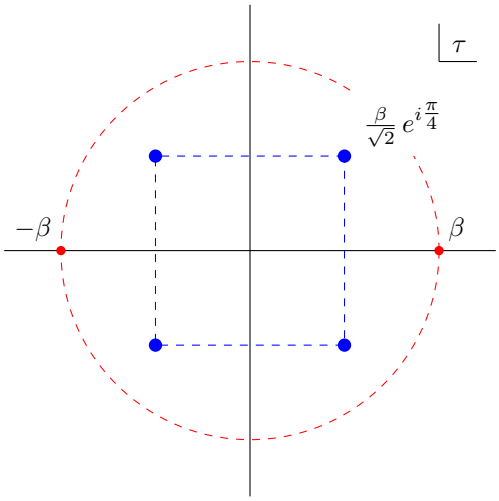

Figure 8. The poles of the stress-tensor sector of the thermal correlator in four dimensions in the complex τ plane. The poles are located inside the circle of radius β.

which, using (3.18), gives

$$\overline{\mathcal{L}}_T \simeq -\frac{1}{\Delta}\log\left[\frac{c(\Delta)\,\Gamma(2\Delta-2)}{4^{(2\Delta-2)}}\,\frac{1}{\tau_c^2}\right]+\frac{2\Delta-2}{\Delta}\log\delta\tau\,. \tag{3.20}$$

If then one inserts the expression (3.14) (including (3.15)) for $c(\Delta)$ then in the large-Δ limit all Δ dependence disappears[24] and

$$\lim_{\Delta\to\infty}\overline{\mathcal{L}}_T \simeq 2\log\delta\tau\,. \tag{3.21}$$

This appears to give the precise form of divergence expected from the bouncing geodesic (2.27).

However, the order of limits for (3.21) is different from that of (2.27). To obtain (3.21), we first focused on the limit $\tau\to\tau_c$ and then took the large Δ limit. On the other hand, the bulk geodesic analysis corresponds to taking the large Δ limit first. That the order of limits is important can be seen from the structure of the Λ_n as functions of Δ, as indicated in figure 3 and 4. To obtain (3.18), we first fixed Δ and analyzed the asymptotic large n behavior of Λ_n, which is in the regime $n > n_* = \Delta/2$. However, the geodesic analysis corresponds to taking first $\Delta\to\infty$, where the cross-over point also goes to infinity, $n_*\to\infty$, and thus we are always in the regime $n < n_*$.

3.4 Asymptotic behavior in the large Δ limit

To properly analyse the large Δ limit and make contact with the geodesic results we first need to take $\Delta\to\infty$ and only then determine the OPE coefficients Λ_n. We show in this subsection that the Euclidean geodesic results (2.10) and (2.12) are indeed recovered.

We begin by expanding the logarithm of (3.10) in small τ

$$\overline{\mathcal{L}}_T = 2\log\tau-\frac{\pi^4}{40}\left(\frac{\tau}{\beta}\right)^4-\frac{(77\Delta^3-483\Delta^2+712\Delta+72)\,\pi^8}{100800\,(\Delta-4)(\Delta-3)(\Delta-2)}\left(\frac{\tau}{\beta}\right)^8+\dots\,. \tag{3.22}$$

[24] At integer values of Δ, the prefactor $c(\Delta)$ diverges (see (3.14)). However, in these cases, one finds $\log(\Delta)/\Delta$ behaviour which vanishes as $\Delta\to\infty$.

JHEP10(2024)105

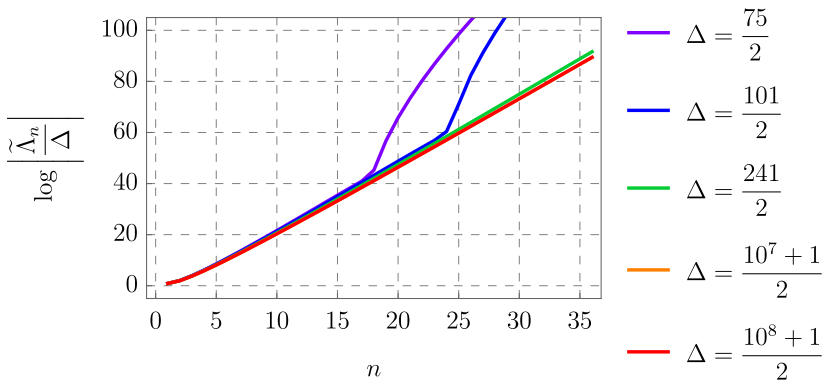

Figure 9. The values of $\log\left|\widetilde{\Lambda}_n/\Delta\right|$ for different Δ. The discrete data is joined for a clearer presentation. When Δ is small, we observe a change of behaviour at $n = n_* = \Delta/2$. For large Δ, this cross-over point disappears and the data converges to a fixed curve, analysed in (3.28).

and compare this with the proper length of the geodesic in Euclidean space (2.13). We see that logarithmic and the τ^4 terms match,[25] while the τ^8 (and all higher order) terms differ. This should not be surprising: the geodesic result can be meaningfully compared to the correlation function only in the $\Delta \to \infty$ limit, in which case

$$\mathcal{L}_T \equiv \lim_{\Delta\to\infty} \overline{\mathcal{L}}_T = 2\log\tau - \frac{\pi^4}{40}\left(\frac{\tau}{\beta}\right)^4 - \frac{11\,\pi^8}{14400}\left(\frac{\tau}{\beta}\right)^8 + \dots\,, \tag{3.23}$$

is equal to (2.13). We checked the agreement explicitly up to order $(\tau/\beta)^{20}$. This importantly shows that in the limit where the conformal dimension of the probe field is large, the stress tensor sector completely reproduces the geodesic result.

When $\Delta \to \infty$, we can also analyse the asymptotic behaviour of the expansion coefficients in $\mathcal{L}_T$. In particular, inserting (3.9) into (3.19), we obtain

$$\overline{\mathcal{L}}_T = 2\log\tau - \sum_{n=1}^{\infty} \frac{\widetilde{\Lambda}_n}{\Delta}\left(\frac{\tau}{\beta}\right)^{4n}\,, \tag{3.24}$$

where $\widetilde{\Lambda}_n$ are appropriate combinations of Λ_n and we have used the fact that $\Lambda_0 = 1$. One can then take the limit $\Delta \to \infty$ as

$$\mathcal{L}_T = \lim_{\Delta\to\infty} \overline{\mathcal{L}}_T = 2\log\tau - \sum_{n=1}^{\infty} L_n \left(\frac{\tau}{\beta}\right)^{4n}\,, \tag{3.25}$$

where we have assumed that one can take the limit inside the series and thus

$$L_n \equiv \lim_{\Delta\to\infty} \frac{\widetilde{\Lambda}_n}{\Delta}\,. \tag{3.26}$$

[25] These terms are related to the exchange of identity and a single stress-tensor operator in the OPE and are fixed by symmetry.

JHEP10(2024)105

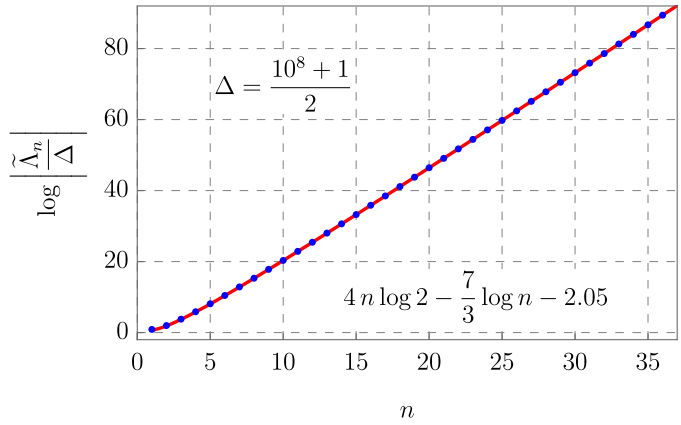

Figure 10. Comparing the holographic data for $\Delta = (10^8+1)/2$ to the ansatz (3.28) and the numerical data given by (3.30).

The first few L_n are given implicitly in (3.23). For higher values of n, we again analyse the data for large but fixed Δ. For some Δ, we plot the values of $\log\left|\widetilde{\Lambda}_n/\Delta\right|$ in figure 9. For small enough Δ, we again observe the cross-over at $n = n_*$ to the asymptotic behaviour analysed in the previous subsection. For large Δ, not only does this cross over get pushed to infinity, but the curve stabilises to an asymptotic value, which we assume is given by

$$\frac{\widetilde{\Lambda}_n}{\Delta} \xrightarrow[\Delta\to\infty]{} L_n + \mathcal{O}\left(\frac{1}{\Delta}\right). \tag{3.27}$$

In practice, we analyse $\Delta = (10^8+1)/2$ and estimate L_n up to $1/\Delta$ corrections. We find that at large values of n, one can make an ansatz

$$L_n = c\, n^b\, a^n \left(1 + \mathcal{O}\left(\frac{1}{n}\right)\right), \tag{3.28}$$

where a, b, and c are all constants. Then for $n \gg 1$

$$\log L_n = \log c + b\,\log n + n\,\log a + \mathcal{O}\left(\frac{1}{n}\right), \tag{3.29}$$

which can be directly fitted to the $\widetilde{\Lambda}_n/\Delta$ data for $\Delta = (10^8+1)/2$ and we find[26] (see also figure 10)

$$\log a = 4\,\log 2 \pm 10^{-6}\,, \qquad b = -\frac{7}{3} \pm 10^{-4} \qquad \log c = -2.050 \pm 10^{-3}\,, \tag{3.30}$$

In what follows we neglect the uncertainties which can be traced back to both $1/\Delta$ and $1/n$ effects. We insert these values into the expansion (3.25) and approximate the sum

[26] We used the data from $n = 10$ to $n = 36$ and used the ansatz (3.28) with up to $1/n^{12}$ corrections.

JHEP10(2024)105

by an integral[27]

$$\mathcal{L}_T \approx 2\log\tau - c\sum_{n=1}^{\infty} n^{-\frac{7}{3}}\, 2^{4n} \left(\frac{\tau}{\beta}\right)^{4n} \approx 2\log\tau - c\int_1^{\infty} dn\, n^{-\frac{7}{3}} \left(\frac{2\,\tau}{\beta}\right)^{4n}$$
$$= 2\log\tau - c\, E_{\frac{7}{3}}\left(-\log\left(\frac{2\tau}{\beta}\right)^4\right). \tag{3.31}$$

This function has a branch cut at all points at which the argument of the logarithm is equal to 1, which is

$$\tau_b = \frac{\beta}{2}\, e^{\frac{i\pi\, k}{2}}, \qquad k \in \mathbb{Z}, \tag{3.32}$$

which suggests four singularities in the complex-τ plane. Focusing on $\tau = \beta/2$, we expand (3.31) around this point and find

$$\mathcal{L}_T \approx -c\,\Gamma\left(-\frac{4}{3}\right)\left(\frac{8}{\beta}\right)^{\frac{4}{3}}\left[\frac{\beta}{2} - \tau\right]^{\frac{4}{3}} + \ldots \approx -1.364\left(\frac{\pi}{2} - \tau\right)^{\frac{4}{3}} + \ldots, \tag{3.33}$$

where we kept only the leading non-analytic behavior at $\tau = \beta/2$, and in the second equality inserted the value of c and taken $\beta = \pi$. The leading non-analytic behavior at $\tau = \beta/2$ of the Euclidean geodesic results (2.10) and (2.12) can be readily found from (2.16), which gives

$$L = -\frac{6^{\frac{4}{3}}}{8}\left(\frac{\pi}{2} - \tau\right)^{\frac{4}{3}} + \ldots \approx -1.363\left(\frac{\pi}{2} - \tau\right)^{\frac{4}{3}} + \ldots\,. \tag{3.34}$$

We see that the asymptotic analysis reproduces the location, the exponent, and the prefactor of the branch point structure observed from bulk geodesics.

One can also study the large Δ limit of the logarithm of the OPE coefficients. One can perform the same analysis as above for a large value of Δ and obtain

$$\log\Lambda_n \sim n\log\Delta - \log\Gamma(n+1) + n\,\log\left(\frac{\pi^4}{40}\right) + \mathcal{O}\left(\frac{1}{\Delta}\right), \tag{3.35}$$

where the numerical value of $\log\left(\frac{\pi^4}{40}\right) \approx 0.89004$ gets reproduced by fitting up to $\approx 10^{-6}$ for $\Delta = (10^8+1)/2$. Exponentiating the above result yields

$$\Lambda_n = \frac{1}{n!}\left(\frac{\Delta\,\pi^4}{40}\right)^n \left(1 + \mathcal{O}\left(\frac{1}{\Delta}\right)\right). \tag{3.36}$$

Inserting this into the OPE and assuming that one can trust these OPE coefficients up to $n \to \infty$ yields

$$G_T(\tau) \approx \frac{1}{\tau^{2\Delta}}\sum_{n=0}^{\infty}\frac{1}{n!}\left(\frac{\pi^4\,\Delta\,\tau^4}{40\,\beta^4}\right)^n \approx \frac{1}{\tau^{2\Delta}}\exp\left[\frac{\pi^4\,\Delta\,\tau^4}{40\,\beta^4}\right], \tag{3.37}$$

[27] We use the function

$$E_n(x) \equiv \int_1^{\infty} t^{-n}\, e^{-t\,x}\, dt\,.$$

JHEP10(2024)105

where we neglected $1/\Delta$ corrections. This result matches [16], where starting from (2.14), a double-scaling limit is taken with $\Delta \to \infty$ while $\tau/\beta \to 0$ such that $\Delta\tau^4/\beta^4$ is held fixed. The significance of this double-scaling limit is that it can be obtained from the exponentiation of the single stress tensor exchange. Indeed, we see that the argument of the exponent is precisely the first non-logarithmic term in the proper length in (2.13). Therefore, taking the large Δ limit at the level of the OPE coefficients neglects all the higher order terms in (3.23), since the information about these terms is encoded in the $1/\Delta$ corrections in (3.36), which are discarded. Since these higher order terms are crucial for the analytic structure of the proper length, we are unable to see the branch cut when taking the $\Delta \to \infty$ limit at the level of the correlation function. As seen above, one needs to analyse the proper length in order to see the branch cut.

3.5 Summary

Here we summarize the main results obtained in this section:

1. For a finite Δ, as indicated by figure 5, $G_T(\tau)$ does not satisfy the KMS condition on its own.

   The double-trace contribution is thus also needed such that the KMS condition is satisfied by the full correlator.

2. For a finite Δ, $G_T(\tau)$ has singular behavior (3.18) at (3.17).

   Full thermal correlation functions cannot have such singular behavior, and thus (3.18) should be cancelled by $G_{[\phi\phi]}(\tau)$. That is, $G_{[\phi\phi]}(\tau)$ must have the same singular behavior, but with an opposite sign.

3. In the $\Delta \to \infty$ limit, the small τ expansion of $\mathcal{L}_T(\tau)$ (defined in (3.23)) precisely recovers the small τ expansion of $L(\tau)$ obtained from gravity.

   While we have only checked the agreement between $\mathcal{L}_T(\tau)$ and $L(\tau)$ in this limit up to τ^{20}, we will assume below that the agreement in fact holds to all orders in the small τ expansion.

4. There is a crossover behavior in Λ_n at $n_* = \Delta/2$. As a result, in the large Δ limit, the singularity of $G_T(\tau)$ at τ_c obtained at a finite Δ is not directly seen, instead we find a branch point singularity in $\mathcal{L}_T(\tau)$ at $\tau = \beta/2$.

   A possible scenario is that as Δ, and therefore n_*, increases the size of the region around $\tau = \tau_c$ where $G_T(\tau)$ diverges shrinks and finally vanishes when $\Delta \to \infty$. At the same time, as Δ increases, the behavior of $\mathcal{L}_T(\tau)$ near $\tau = \beta/2$ gets closer and closer to the singular behavior observed in the geodesic analysis (3.33). This would be another signature of the noncommutativity of limits $\tau \to \tau_c$ and $\Delta \to \infty$.

4 Boundary interpretation of the gravity results

We now use the results obtained from the OPE analysis of section 3 to interpret the gravity results reviewed in section 2. While the singular behavior (3.18) has the same form as that

JHEP10(2024)105

in (1.2), the connection is not immediate, as (3.18) and (1.2) appear in different quantities and in different regimes (one in G_T at finite Δ, while the other in $\hat{G}$ at infinite Δ). What is more, as discussed at the end of last section, the singular behavior (3.18) disappears in the large Δ limit, which obscures its connection to the bouncing singularities and black hole singularities.

In this section, we argue that the singular behavior (3.18) can indeed be identified as the boundary origin of (1.2) and thus the black hole singularities. Below we will restore β, and when we say "for all τ" it always refers to $\mathrm{Re}\,\tau \in (0, \beta)$.

4.1 Role of the double-trace contributions in the large Δ limit

We first discuss the role of the double-trace contributions in the large Δ limit. In section 3 we found that in the $\Delta \to \infty$ limit, the small τ expansion of $\mathcal{L}_T(\tau)$ precisely recovers that of $L(\tau)$ obtained from the geodesic analysis (i.e. item 3 of section 3.5). Furthermore, we have shown that in the large Δ limit, $\mathcal{L}_T(\tau)$ has a branch point singularity of the form $(\frac{\beta}{2} - \tau)^{\frac{4}{3}}$ at $\tau = \beta/2$. That is, for large Δ, $\mathcal{L}_T(\tau)$ (and $L(\tau)$) has a radius of convergence $\beta/2$, and the double-trace contribution $G_{[\phi\phi]}(\tau)$ can be neglected in the large Δ limit for $\tau < \beta/2$.

That $G_{[\phi\phi]}(\tau)$ can be neglected for small τ has a simple explanation from the OPE structure. The double-trace contribution $G_{[\phi\phi]}(\tau)$ has a small τ OPE of the form

$$G_{[\phi\phi]}(\tau) = \frac{1}{\beta^{2\Delta}} \sum_{k=0}^{\infty} D_k \left(\frac{\tau}{\beta}\right)^{2k} \tag{4.1}$$

where D_k are some constants. The appearance of even powers in (4.1) comes from the fact that the double-trace operators $\phi(\partial^2)^n \partial_{i_1} \cdots \partial_{i_l} \phi$ have dimensions $2\Delta + 2n + l$ and only the ones with even l can have nonzero thermal expectation values in (1.7).

Comparing (4.1) with the analogous expression for the stress tensor sector (3.9) gives

$$\frac{G_{[\phi\phi]}(\tau)}{G_T(\tau)} \sim \left(\frac{\tau}{\beta}\right)^{2\Delta} \left(1 + \mathcal{O}\left(\tau^2\right)\right), \tag{4.2}$$

with the full $G(\tau)$ having the structure

$$G(\tau) = \frac{1}{\tau^{2\Delta}} \left[\sum_{n=0}^{\infty} \Lambda_n \left(\frac{\tau}{\beta}\right)^{dn} + \sum_{k=0}^{\infty} D_k \left(\frac{\tau}{\beta}\right)^{2k+2\Delta}\right]. \tag{4.3}$$

We may conclude from the above equation that, in the large Δ limit, the double-trace contribution is always suppressed for all τ. This, however, assumes that we can take the large Δ limit *inside* the sum, which requires $G(\tau)$ to be uniformly convergent for all Δ for all τ. This is incorrect, since as mentioned earlier, $\mathcal{L}_T(\tau)$ develops a branch point singularity at $\tau = \beta/2$ in the large Δ limit, and only has the radius of convergence equal to $\frac{\beta}{2}$.[28] Thus for $|\tau| \geq \beta/2$, we need to sum the series for $G(\tau)$ first for finite Δ and then take the large Δ limit.

For $|\tau| \geq \beta/2$, we expect $G_{[\phi\phi]}(\tau)$ will be needed. After all, as mentioned earlier, the double-trace contributions are needed for the full correlator to satisfy the KMS condition. Now comparing with the discussion of section 2.2, we can identify

$$\mathcal{L}_T(\tau) = L(\widetilde{E}_0(\tau)) \tag{4.4}$$

[28] Even if the series $G_T(\tau)$ remains convergent in the large Δ limit for all τ, it is possible that the full series $G(\tau)$ may not be uniformly convergent for all Δ for all τ. We will see an example of this in section 4.4.

JHEP10(2024)105

where L on the r.h.s. is the geodesic distance obtained from gravity. From (2.18), we can further identify

$$\mathcal{L}_{[\phi\phi]}(\tau) = L(\widetilde{E}_1(\tau)) \tag{4.5}$$

which becomes important for $\theta \leq -\frac{\pi}{2}$, with θ defined as $\frac{\beta}{2} - \tau = re^{i\theta}$. Furthermore, the relative dominance between $\widetilde{E}_0$ and $\widetilde{E}_1$ saddles discussed there can now be written in terms of the boundary language as

$$\lim_{\Delta\to\infty} G(\tau) = \lim_{\Delta\to\infty} \begin{cases} G_T(\tau) & \tau < \frac{\beta}{2} \\ G_{[\phi\phi]}(\tau) & \tau > \frac{\beta}{2} \\ G_T(\tau) + G_{[\phi\phi]}(\tau) & \tau = \frac{\beta}{2} + it_L,\ t_L \in \mathbb{R} \end{cases} . \tag{4.6}$$

In particular, $G_T(\tau)$ and $G_{[\phi\phi]}(\tau)$ correspond respectively to the contributions from the two complex geodesics on the gravity side.

One can ask why the uniform convergence stops at $\tau = \beta/2$. If we consider a theory with time-reversal symmetry, $\tau \to -\tau$, that satisfies the KMS condition, $G(\tau) = G(\beta - \tau)$, then the branch point at which the OPE sum and the $\Delta \to \infty$ limit cannot be exchanged can be in principle at any $0 \leq \beta^* \leq \beta/2$. It would be interesting to explore this direction further.

4.2 Boundary interpretation of the bouncing singularities

We now turn to the boundary interpretation of the bouncing singularities (1.2).

The identification (4.4) is consistent with our numerical observation that the singular behavior (3.18) is not directly seen in the large Δ limit, as $\widetilde{E}_0$ corresponds to a complex geodesic for $\tau = \beta/2 + it_L$, and is regular at $\tau_c = \frac{\beta}{2}(1+i)$. The same statement applies to $G_{[\phi\phi]}(\tau)$. As we discussed in item (2) of section 3.5, at a finite Δ, $G_{[\phi\phi]}(\tau)$ should also have a bouncing singularity at τ_c, but the identification (4.5) implies that the singularity is no longer there in $\mathcal{L}_{[\phi\phi]}(\tau)$. Nevertheless, we would like to argue that the bouncing geodesic singularities (1.2) do originate from (3.18).

More explicitly, after obtaining $G_T(\tau)$ from the OPE of multiple stress tensors, we can expand $\mathcal{L}_T(\tau)$ near $\tau = \beta/2$ as

$$\mathcal{L}_T(\tau) \sim \left(\frac{\beta}{2} - \tau\right)^{\frac{4}{3}} + \ldots \equiv f_T(y)\,, \quad y \equiv \left(\frac{\beta}{2} - \tau\right)^{\frac{1}{3}}\,, \tag{4.7}$$

where we neglect the constant prefactor and terms that are regular at $\tau = \beta/2$. Since on the gravity side $\tilde{E}_1(\tau)$ and $\tilde{E}_2(\tau)$ are related to $\tilde{E}_0(\tau)$ by phase multiplications (2.17), we can then write

$$\mathcal{L}_{[\phi\phi]}(\tau) = f_T\left(e^{-\frac{2\pi i}{3}} y\right), \quad \hat{\mathcal{L}}(\tau) = f_T\left(e^{-\frac{4\pi i}{3}} y\right)\,. \tag{4.8}$$

That is, through the branch point singularity developed by $\mathcal{L}_T(\tau)$ at $\tau = \beta/2$, both $\mathcal{L}_{[\phi\phi]}(\tau)$ coming from $G_{[\phi\phi]}(\tau)$, and $\hat{\mathcal{L}}(\tau)$ (2.27) corresponding to the bouncing geodesic are fully determined from $\mathcal{L}_T(\tau)$.

While the singular behavior (3.18) of $G_T(\tau)$ and $G_{[\phi\phi]}(\tau)$ have seemingly both disappeared in themselves in the large Δ limit, the bouncing singularities are not lost, but are transferred

JHEP10(2024)105

to $\hat{\mathcal{L}}(\tau)$. They are just not as manifest. This phenomenon is quite remarkable. As emphasized in section 3, the bouncing singularities of $G_T(\tau)$ at finite Δ are controlled by the asymptotic large n behavior in the regime $n > n_*$, while $\mathcal{L}_T(\tau)$ is given by Λ_n in the regime $n < n_*$ after first taking $n_* \to \infty$. Nevertheless, $\mathcal{L}_T(\tau)$ does contain the information regarding the bouncing singularities, albeit indirectly.

At finite Δ, both $G_T(\tau)$ and $G_{[\phi\phi]}(\tau)$ have bouncing singularities, then why do we say that they originate from the stress tensor sector, not from the double-trace sector? We already saw that in the large Δ limit, both $\mathcal{L}_{[\phi\phi]}(\tau)$ and $\hat{\mathcal{L}}(\tau)$ are determined from $\mathcal{L}_T(\tau)$. This is not an accident; in fact, $G_{[\phi\phi]}(\tau)$ is also determined by $G_T(\tau)$ for any Δ.

To make the point clear, recall the OPE computation of a vacuum four-point function

$$\langle 0|VVWW|0\rangle = \sum_O C_{VVO} C_{WWO} \langle 0|OO|0\rangle \,, \tag{4.9}$$

where the four-point function is fully determined from the OPE data and vacuum two-point functions. In contrast, in the OPE computation (1.7) of $G(\tau)$, the right hand side of the equation involves the thermal expectation values of double-trace operators

$$\left\langle \phi(\partial^2)^n \partial_{i_1} \cdots \partial_{i_l} \phi \right\rangle_\beta \tag{4.10}$$

whose values require knowledge of thermal two-point functions of ϕ, which are just $G(\tau) = \langle \phi(\tau)\phi(0)\rangle_\beta$ (and derivatives thereof) evaluated at a fixed point. These two-point functions are unknown but necessary in order to determine the OPE expansion. In other words, both sides of (1.7) depend on $G(\tau)$, and it should be viewed as an equation *to solve* for $G(\tau)$, rather than as an expression to calculate the left hand side as is the case for (4.9). The inputs that we need to solve (1.7) are $G_T(\tau)$, the OPE coefficients of $\phi(\partial^2)^n \partial_{i_1} \cdots \partial_{i_l} \phi$, as well as imposing that $G(\tau)$ obeys the KMS condition and be analytic in $\mathrm{Re}\,\tau \in (0, \beta)$. Thus we can say $G(\tau)$ and $G_{[\phi\phi]}(\tau)$ are determined from $G_T(\tau)$.

Finally, we comment that $G_T(\tau)$ is closely connected to the bulk geometry, and thus enjoys some level of universality. The OPE coefficients for k-stress tensor exchanges correspond in the bulk to couplings of the bulk dual Φ of ϕ to multiple gravitons, i.e. couplings of the form $\Phi\Phi h^k$, where h schematically denotes the bulk graviton. The thermal one-point function v_n for k stress tensors is given schematically by $(\langle T_{\mu\nu}\rangle_\beta)^k$, i.e. k-th power of the boundary stress tensor in the black hole geometry.

4.3 A speculation on the momentum space behavior and bouncing singularities

Now suppose the behavior (1.5) is also present at finite Δ. Then given (3.18), it is tempting to speculate that

$$G(i\omega_E) \sim \int_{-\infty}^{\infty} d\tau\, e^{i\omega_E \tau}\, G_T(\tau) \,. \tag{4.11}$$

We use $\sim$ in the above equation to indicate that while (under some assumptions) the right hand side gives the correct qualitative behavior for $G(i\omega_E)$ in the limit $\omega_E \to \pm\infty$, at the moment we do not have enough information to specify a precise relation. As $\omega_E \to +\infty$, we assume the behavior of $G_T(\tau)$ at infinity is such that we can close the contour in the

JHEP10(2024)105

upper half complex τ-plane. Then the integral will mainly receive contributions from the neighborhood of $\tau_c^+ = \frac{\beta}{2} + i\frac{\widetilde{\beta}}{2}$, leading to

$$G(i\omega_E) \sim e^{i\omega_E \tau_c} \omega_E^{2\Delta-3} \propto (i\omega_E)^{2\Delta-3} e^{i(i\omega_E)t_c^+}, \quad \omega_E \to +\infty \,. \tag{4.12}$$

Similarly, for $\omega_E \to -\infty$, we close the contour in the lower half complex τ-plane, with the main contribution coming from integration around $\tau_c^- = \frac{\beta}{2} - i\frac{\widetilde{\beta}}{2}$, leading to

$$G(i\omega_E) \sim (i\omega_E)^{2\Delta-3} e^{i(i\omega_E)t_c^-}, \quad \omega_E \to -\infty \,. \tag{4.13}$$

4.4 Double-trace contributions in the GFF example

Now consider the following example

$$G(\tau)^{(GFF)} = \langle \phi(\tau)\phi(0) \rangle_\beta^{(GFF)} = \sum_{m\in\mathbb{Z}} \frac{1}{(\tau + m\,\beta)^{2\Delta}} \,, \tag{4.14}$$

which is obtained by taking the vacuum Euclidean two-point function of ϕ and adding images in the τ direction such that it has periodicity β. The $m = 0$ term is the contribution of the identity while all other terms correspond to multi-trace contributions [47, 48], as expanding $m \neq 0$ terms in τ we find a power series of the form (4.1). It will also be convenient to define

$$\mathcal{L}(\tau)^{(GFF)} = -\lim_{\Delta\to\infty} \frac{1}{\Delta} \log G(\tau)^{(GFF)} \tag{4.15}$$

It is easy to compute $\mathcal{L}(\tau)^{(GFF)}$: it is given by

$$\mathcal{L}(\tau)^{(GFF)} = 2\log\tau, \ \tau < \frac{\beta}{2}, \qquad \mathcal{L}(\tau)^{(GFF)} = 2\log(\beta - \tau), \ \tau > \frac{\beta}{2} \tag{4.16}$$

and has a cusp at $\tau = \beta/2$.

We will see momentarily that the series in τ which defines $\frac{1}{\Delta}\log G(\tau)^{(GFF)}$ is uniformly convergent for all Δ only for $\tau < \beta/2$. Moreover, the GFF example satisfies (4.6), which also applies in holography. It will be convenient to write

$$-\frac{1}{\Delta}\log G(\tau)^{(GFF)} = 2\log\tau - \frac{1}{\Delta}\log\left(1 + \sum_{m\neq 0} \frac{\tau^{2\Delta}}{(\tau + m\beta)^{2\Delta}}\right) \tag{4.17}$$

where we have separated the $m = 0$ term (the identity operator contribution). We can now expand the second term for small τ,

$$-\frac{1}{\Delta}\log G(\tau)^{(GFF)} = 2\log\tau + \lim_{n\to\infty} \mathcal{L}^{(n)}(\tau), \qquad \mathcal{L}^{(n)}(\tau) = \sum_{k=0}^{n} c_k(\Delta) \left(\frac{\tau}{\beta}\right)^{2\Delta+2k} \tag{4.18}$$

where we have written the infinite series as a limit. Taking the large Δ limit inside the series amounts to the order of limits

$$\lim_{n\to\infty} \lim_{\Delta\to\infty} \mathcal{L}^{(n)}(\tau) = 0, \qquad \tau < \beta \,, \tag{4.19}$$

JHEP10(2024)105

in which case all terms vanish. However, the limits $n \to \infty$ and $\Delta \to \infty$ may not be exchangeable. For the other order of limits, we should take the large Δ limit directly in (4.17), which gives

$$\lim_{\Delta\to\infty} \lim_{n\to\infty} \mathcal{L}^{(n)}(\tau) = \begin{cases} 0, & \tau < \frac{\beta}{2} \\ -2\log\tau + 2\log(\beta-\tau), & \tau > \frac{\beta}{2} \end{cases} . \tag{4.20}$$

By comparing (4.19) and (4.20) we see that the limits can only be exchanged when $\tau < \beta/2$. From the Moore-Osgood theorem, it follows that the limit $n \to \infty$ (the OPE) cannot be uniformly convergent in Δ for $\tau > \beta/2$. This example nicely illustrates the role of double traces: when τ is small, only the stress-tensor sector (identity) contributes in the large-Δ limit and the double traces can be safely ignored. When $\tau > \beta/2$, the double trace contribution dominates.

Furthermore, for $\tau = \frac{\beta}{2} + it_L, t_L \in \mathbb{R}$ at large Δ terms with $m = 0$ and $m = -1$ both contribute

$$G^{(GFF)}\left(\tau = \frac{\beta}{2} + it_L\right) \approx \frac{1}{\tau^{2\Delta}} + \frac{1}{(\tau-\beta)^{2\Delta}} . \tag{4.21}$$

We thus see the GFF example (4.14) has exactly the same behavior as (4.6) except that $G_T(\tau)$ only has contribution from the identity and thus is always trivially convergent for all τ even in the large Δ limit.

5 Discussion

We showed that the stress tensor sector of the thermal two-point function of scalar operators exhibits bouncing singularities at finite Δ. We argued that this singular behavior matches the one observed in [8] from the bulk geodesic analysis, and can be interpreted as a boundary reflection of black hole singularities. Since contributions from multi-stress tensor exchanges do not depend on the specific details of the operators, they encode the universal features of black hole singularities as probed by generic bulk fields. Furthermore, we expect that two-point functions of general "light" operators in generic "heavy" states exhibit thermal behavior at leading order in the $1/N$ expansion. Hence our conclusion can also be used to explain the universality of black hole singularities in single-sided black holes formed from gravitational collapse.

Our results also help elucidate the role of double-trace operator contributions, and in particular connect them to geodesic results in the limit of large conformal dimensions.

Below we first discuss results in other dimensions, then give a boundary interpretation of the gravity results for the boundary on a sphere, and finally offer some future perspectives.

5.1 Other spacetime dimensions

In the main text, we have focused on $d = 4$ for definiteness. Here we discuss the results in other dimensions.

For $d = 2$, which is discussed in detail in appendix D, Euclidean function $G(\tau, x)$ (including the spatial dependence) is known exactly from conformal symmetry, and can be shown to

JHEP10(2024)105

solely come from the Virasoro descendants of the identity, which are the multi-stress operators. The stress tensor sector satisfies the KMS condition by itself, and does not have any unphysical singularity. The corresponding bulk geometry is described by the AdS Rindler, and there is no singularity behind the Rindler horizon.

The $d = 4$ discussion of the main text can be straightforwardly generalized to $d = 6$ and $d = 8$. The geodesic analysis of [8] yields the bouncing singularities for general d at

$$\tau_c = \frac{\beta}{2} \pm i\frac{\beta}{2}\,\frac{\cos\frac{\pi}{d}}{\sin\frac{\pi}{d}} = \pm i\frac{\beta e^{\mp\frac{i\pi}{d}}}{2\sin\frac{\pi}{d}}\ . \tag{5.1}$$

As discussed in appendix G, these singularities are exactly reproduced from the asymptotic analysis of the stress tensor OPE in $d = 6$ and $d = 8$, with the behavior near the singularities

$$G_T(\tau) \propto \frac{1}{(\delta\tau)^{2\Delta-\frac{d}{2}}}, \quad \delta\tau = \tau_c - \tau\ . \tag{5.2}$$

The $-\frac{d}{2}$ term in the exponent $2\Delta - \frac{d}{2}$ is somewhat curious and it would be interesting to understand its meaning further.

Note that for $d = 6$, $|\tau_c| = \beta$, while for $d = 8$, $|\tau_c| > \beta$, which again highlights that the stress tensor sector contribution $G_T(\tau)$ does not obey the KMS condition. It is also curious to note that for both $d = 6$ and $d = 8$ there are additional singularities other than (5.1) (or their reflection in the left τ plane) at

$$d = 6: \qquad \tau = \beta, \tag{5.3}$$

$$d = 8: \qquad \tau = \frac{\beta}{2}\frac{e^{\pm i\frac{\pi}{8}}}{\sin\frac{\pi}{8}}\,, \tag{5.4}$$

These singularities have $\mathrm{Re}\,\tau > \beta/2$. It would be interesting to see whether they play a role similar to the bouncing singularities.

5.2 Boundary theory on a sphere

Consider the boundary CFT on a sphere S^{d-1} of radius R for $d > 2$. The decomposition (1.8) still applies but the structure of each term becomes significantly more complicated. For example, now the descendants of the multiple stress tensor operators can also contribute, and there is a new dimensionless parameter $\frac{\beta}{R}$. Nevertheless, we expect that the boundary theory interpretation we gave in this paper should still apply qualitatively. That is, there should be singularities in the stress tensor sector contribution $G_T(\tau)$ at a general finite Δ, which in the large Δ limit, "become" the bouncing singularities seen in the geodesic analysis. Below we give a boundary interpretation of the gravity analysis given in section 3.3 of [8].

Figure 11 gives Euclidean time separation τ as a function of $\widetilde{E}$ obtained from bulk Euclidean geodesics. In contrast with (2.16), at $\tau = \beta/2$, there are three different real solutions of $\widetilde{E}$, labelled as $\widetilde{E}_0, \widetilde{E}_1, \widetilde{E}_2$ in the figure. Contribution from the $\widetilde{E}_0$ branch, which is the unique real solution for sufficiently small τ, should again be identified with the large Δ limit of $\mathcal{L}_T$. Contribution from the $\widetilde{E}_1$ branch should be identified with the double trace contributions $\mathcal{L}_{[\phi\phi]}$, while the middle branch $\widetilde{E}_2$ (in gray) does not contribute and gives rise to the bouncing geodesics when extended to complex $\tau = \frac{\beta}{2} + it_L$. $\widetilde{E}_0, \widetilde{E}_1$ again correspond

JHEP10(2024)105

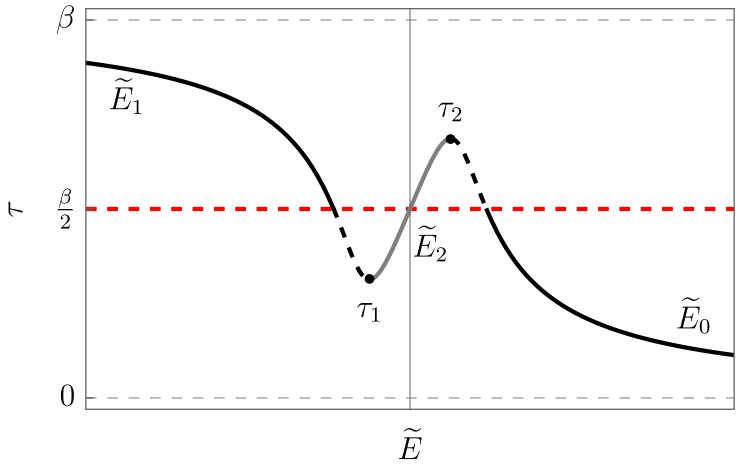

Figure 11. τ as function of $\widetilde{E}$ obtained from the Euclidean geodesic analysis for the boundary theory on a sphere.

to complex geodesics for such complex τ. The geodesic saddle $\widetilde{E}_1$ corresponding to the double-trace piece starts appearing at some value $\tau_1 < \beta/2$ (denoted with a dot in figure 11), but is subdominant for $\tau < \beta/2$. Its contribution becomes the same as that from $\widetilde{E}_0$ at $\tau = \beta/2$. For $\tau > \beta/2$, $\widetilde{E}_1$ (i.e. the double-trace piece) dominates. We see that the structure is identical to (4.6).

In the large Δ limit, $\mathcal{L}_T(\tau)$ is now analytic at $\beta/2$, but develops a square root branch point singularity at some value $\tau_2 > \beta/2$ (see figure 11). Near $\tau = \tau_2$, the geodesic distance $\hat{\mathcal{L}}(\tau)$ corresponding to $\widetilde{E}_2$ branch can be obtained from $\mathcal{L}_T$ as follows,

$$\mathcal{L}_T(\tau) = f_T(y), \quad y \equiv (\tau_2 - \tau)^{\frac{1}{2}}, \quad \hat{\mathcal{L}}(\tau) = f_T(-y) \ . \tag{5.5}$$

Analytically continuing $\hat{\mathcal{L}}(\tau)$ to complex $\tau = \frac{\beta}{2} + it_L$ should yield the bouncing singularities. In this case, the double-trace piece $\mathcal{L}_{[\phi\phi]}$ is still determined from $\mathcal{L}_T(\tau)$ through a more involved procedure. After finding $\hat{\mathcal{L}}(\tau)$ from $\mathcal{L}_T(\tau)$ at τ_2 using (5.5), we continue $\hat{\mathcal{L}}(\tau)$ to τ_1, where $\hat{\mathcal{L}}(\tau)$ should encounter another square root branch point singularity. At τ_1 we can obtain $\mathcal{L}_{[\phi\phi]}(\tau)$ from $\hat{\mathcal{L}}(\tau)$ using a parallel procedure as (5.5).

5.3 Future perspectives

Here we comment on some immediate extensions of our results and other future directions:

1. **Subleading corrections and spatial dependence.**

   One can try to go a step further and analyze subleading corrections and spatial dependence to the leading singular behavior we found in $G_T(\tau)$ — we discuss corrections in $\delta\tau$ in appendix E and the corrections in small x in appendix F. Our current analysis is not enough for drawing further conclusions. We also analyzed the contributions of lowest-twist operators in the stress-tensor sector. We summarise our early analysis in appendix H. Interestingly, we find that the leading twist OPE coefficients grow quicker than the Λ_n coefficients (which contain contributions from the $[T_{\mu\nu}]^n$ operators

JHEP10(2024)105

of all twist) at large n and furthermore do not exactly reproduce the locations of the bouncing singularities. This shows that the leading-twist exchanges are not the dominant exchanges in the stress-tensor sector and that the subleading twists are crucial to reproduce the singular behavior.

2. **Leading twist OPE.**

   It is not surprising that the resummation of the leading twist contributions does not lead to the correct bouncing singularities. The kinematical regime where the leading twist contributions are dominant is the near-lightcone regime, where $x^- \to 0$ with $x^-(x^+)^3/\beta^4$ fixed. Clearly, this regime is very different from the $\vec{x} = 0$ kinematics discussed in this paper. The near-lightcone limit has its advantages — the OPE coefficients are universal [24] and, furthermore, can be computed using CFT bootstrap [23]. In addition, the geodesic analysis in this limit takes a simple form [42]. One may hope that generalization of the results of the present paper to the near-lightcone regime may provide a useful way of computing analytic observables which can probe black hole singularities.

3. **Nature of singularities of BTZ black holes?**

   For $d = 2$, when the spatial direction is a circle, the bulk system is described by a BTZ black hole, which has an orbifold singularity. The singularity is invisible to the kind of geodesic analysis reviewed in section 2, and thus to the kind of boundary correlation functions discussed in this paper. The singularity is, however, visible from correlation function of the form

   $$\langle \Phi(X)\phi(0,0)\rangle_\beta \tag{5.6}$$

   when the bulk point X is taken to the black hole singularity [55] (here $\Phi(X)$ is the bulk field dual to boundary operator ϕ). $\Phi(X)$ can be expressed in terms of boundary operators using bulk reconstruction, and thus (5.6) can be written in terms of boundary correlation functions. It would be interesting to see whether it is possible to understand the nature of the BTZ singularities in terms of features of the stress tensor or double-trace contributions to the thermal correlation functions.

4. **OPE structure for the boundary CFT on a sphere.**

   It would be desirable to use the stress tensor sector for the CFT on a sphere for $d > 2$ to check explicitly whether the bouncing singularities can be recovered and whether the radius of convergence of the stress-tensor sector at large Δ is larger than $\beta/2$. For this purpose one can use the results of [24] for a spherical black hole geometry and repeat our analysis.

5. **Effects on the black hole singularities from α' or G_N corrections.**

   Connecting black hole singularities to the singularities of the stress tensor sector of boundary thermal correlators opens up new avenues for understanding effects on the

JHEP10(2024)105

black hole singularities from α' or G_N corrections, and their possible resolutions at finite α' or G_N.[29]

We will use the example of $\mathcal{N}=4$ super-Yang-Mills theory with gauge group SU(N) as an illustration, for which α' and G_N translates into $1/\sqrt{\lambda}$ and $1/N^2$, where λ is the 't Hooft coupling.

Consider first a finite, but large λ in the large N limit, so that we can still talk about bulk gravity in terms of spacetime geometry. In this case, there are two important changes: (i) The coefficients Λ_n in (3.9) become λ-dependent [26]. (ii) At finite λ, single-trace operators other than the stress tensor, which can include light operators dual to other supergravity fields and operators corresponding to stringy modes, may develop nonzero thermal expectation values, and can contribute to the exchanges in (1.7). More explicitly, suppose the thermal expectation value of a single-trace operator O is nonzero at finite λ, and O appears in the OPE expansion of $\phi(\tau)\phi(0)$, then in (1.8) we should add contributions from the exchanges of O^n for $n \in \mathbb{N}$. Denote such a contribution as $G_O(\tau)$, and we should sum over all possible such $G_O(\tau)$.

(i) arises from λ-dependence of the OPE coefficients as well as the λ-dependence of the thermal expectation value of the stress tensor. These corrections could change the location of the bouncing singularities we saw in $G_T(\tau)$, and can in principle be studied perturbatively in $1/\sqrt{\lambda}$ expansion. (ii) will make the connection of the singularities in G_T to spacetime singularities discussed in section 4 more intricate. For example, in the large Δ limit, both $G_T(\tau)$ and $G_O(\tau)$ may contribute in the small τ regime, with the contribution from G_O interpreted as smearing of geodesics from interacting with stringy excitations.

At finite N (i.e. finite G_N in the bulk), equation (1.8) no longer applies. Neither the notion of multiple stress tensor nor double-trace operators make exact sense. But in the large N limit, it should be possible to study perturbative $1/N$ corrections to $G_T(\tau)$, and could lead to insights into the nature of the black hole singularities under perturbative G_N corrections.

6. **Black hole in the presence of matter fields.**

In this paper we considered the simplest Schwarzschild black hole. It is interesting to consider solutions with matter fields turned on which can deform the black hole interior as well as the region near the black hole singularities (see e.g. [57] for an example). On the boundary side, this corresponds to turning on marginal or relevant deformations. It would be interesting to see whether the stress energy sector still captures the bouncing singularities.

Similarly, one can consider a spacetime corresponding to a spherically symmetric star. The spacetime would still be described by the Schwarzschild metric outside the star's radius, which is greater than the horizon radius of a black hole with equal mass, while the star's interior would depend on the matter field configuration. It would be interesting

[29] An alternative approach addressing black hole singularities in higher derivative gravity can be found for example in [56] and references therein.

JHEP10(2024)105

to see how our results are altered in this case, especially because such a star solution is free of curvature singularities.

Since the stress-tensor sector is determined solely from the asymptotic expansion of the bulk equations of motion and the star and black hole spacetimes are asymptotically identical, the stress-tensor sector contributions to the OPE would be identical as well. As such, one can speculate that all the details about the matter content and the star's interior will be contained within the double-trace sector.

However, a hidden working assumption used in this paper is that the near-boundary expansion provides a reliable solution to the Klein-Gordon equation in the region $r \in (0, \infty)$. For a Schwarzschild-AdS solution this is justified since the spacetime is analytic everywhere apart from the singularity at $r = 0$. For solutions with matter fields, this is no longer the case, since the Schwarzschild metric ceases to be the valid description at a non-zero radius $R_0 > 0$ (radius of the star), where a discontinuity in the metric appears. One might thus question the validity of the method in this case. It would be interesting to resolve this issue in detail.

7. **Possible boundary origin of the BKL behavior.**

   In the presence of perturbations, there can be intricate chaotic dynamics in the approach to the black hole singularities [58, 59], called the BKL or mixmaster behavior. Recently, such chaotic behavior has been obtained inside a four dimensional asymptotically AdS planar black hole [60]. The connection between the black hole singularities and multiple stress tensor exchange on the boundary should be helpful to understand the boundary origin of the chaotic behavior.

Acknowledgments

We would like to thank I. Araya, S. Collier, M. Dodelson, C. Esper, S. Hartnoll, L. Iliesiu, D. Jafferis, R. Karlsson, D. Kolchmeyer, M. Kulaxizi, A. Levine, J. Maldacena, K. Skenderis, S. Solodukhin, J. Sorce, S. Zhiboedov for discussions. The work of NČ and AP is supported in part by the Science Foundation Ireland under the grant agreement 22/EPSRC/3832. SV was supported in part by the Irish Research Council Government of Ireland Postgraduate Fellowship under project award number GOIPG/2023/3661. HL is supported by the Office of High Energy Physics of U.S. Department of Energy under grant Contract Number DE-SC0012567 and DE-SC0020360 (MIT contract # 578218). NČ, AP and SV thank Mainz Institute for Theoretical Physics, where part of this work was completed, for hospitality. AP also thanks Harvard University, where part of this work was completed, for hospitality.

A Structure of the correlation functions

In this appendix we discuss the stress-tensor sector of the thermal two-point function of scalar operators (3.1). The contribution of the n-stress tensor $(T_{\mu\nu})^n$ to the correlator is, up to a constant, the $(T_{\mu\nu})^n$ conformal partial wave[30] (CPW) of the heavy-heavy-light-light

[30] Here, we are referring to conformal partial waves as defined in [61, 62]. Note that in modern CFT literature this term is sometimes used in a different context.

JHEP10(2024)105

(HHLL) correlator on $\mathbb{R}\times S_R^{d-1}$ [63]. Light and heavy refer to how the conformal dimensions of the inserted operators scale with the central charge, C_T, of the CFT. The conformal dimension of the light operator, Δ, does not scale with the central charge, while for the heavy operator it does, $\Delta_H \sim \mathcal{O}(C_T)$.

Starting in flat space, the HHLL four-point function can be expanded in the corresponding CPWs $\widehat{W}_{\Delta',J'}$ as

$$G(z,\bar{z}) \equiv \langle \mathcal{O}_H(0)\phi(z,\bar{z})\phi(1)\mathcal{O}_H(\infty)\rangle = \sum_{\Delta',J'} c_{\Delta',J'}\widehat{W}_{\Delta',J'}\,, \tag{A.1}$$

where the sum runs over all primaries and $c_{\Delta',J'}$ is a combination of OPE coefficients. The flat space CPW are given by [61, 62][31]

$$d=2 \quad \widehat{W}_{\Delta',J'} = \frac{1}{(Z\overline{Z})^{\Delta}}\Big(k_{\Delta'+J'}(Z)k_{\Delta'-J'}(\overline{Z}) + k_{\Delta'-J'}(Z)k_{\Delta'+J'}(\overline{Z})\Big) \tag{A.2}$$

$$d=4 \quad \widehat{W}_{\Delta',J'} = \frac{1}{(Z\overline{Z})^{\Delta}}\frac{Z\overline{Z}}{Z-\overline{Z}}\Big(k_{\Delta'+J'}(Z)k_{\Delta'-J'-2}(\overline{Z}) - k_{\Delta'-J'-2}(Z)k_{\Delta'+J'}(\overline{Z})\Big) \tag{A.3}$$

$$\begin{aligned} d=6 \quad \widehat{W}_{\Delta',J'} = \frac{1}{(Z\overline{Z})^{\Delta}}\Big(&\mathcal{F}_{0,0}(Z,\overline{Z}) - \frac{J'+3}{J'+1}\mathcal{F}_{-1,1}(Z,\overline{Z}) \\ &- \frac{(\Delta'-4)(\Delta'+J')^2}{16(\Delta'-2)(\Delta'+J'+1)(\Delta'+J'-1)}\mathcal{F}_{1,1}(Z,\overline{Z}) \\ &+ \frac{(\Delta'-4)(J'+3)}{(\Delta'-2)(J'+1)}\frac{(\Delta'-J'-4)^2}{16(\Delta'-J'-5)(\Delta'-J'-3)}\mathcal{F}_{0,2}(Z,\overline{Z})\Big)\,, \end{aligned} \tag{A.4}$$

where

$$k_\eta(\xi) = \xi^{\frac{\eta}{2}}\,{}_2F_1(\tfrac{\eta}{2},\tfrac{\eta}{2},\eta,\xi)\,, \tag{A.5}$$

$$\mathcal{F}_{n,m}(Z,\overline{Z}) = \frac{(Z\overline{Z})^{\frac{1}{2}(\Delta'-J')}}{(\overline{Z}-Z)^3}(\mathbb{F}_{n,m}(Z,\overline{Z}) - \mathbb{F}_{n,m}(\overline{Z},Z))\,, \tag{A.6}$$

$$\begin{aligned} \mathbb{F}_{n,m}(Z,\overline{Z}) = \overline{Z}^{J'+n+3}Z^m\,{}_2F_1\Big(\frac{\Delta'+J'}{2}+n,\frac{\Delta'+J'}{2}+n;\Delta'+J'+2n;\overline{Z}\Big) \\ \times\,{}_2F_1\Big(\frac{\Delta'-J'}{2}-3+m,\frac{\Delta'-J'}{2}-3+m;\Delta'-J'-6+2m;Z\Big)\,. \end{aligned} \tag{A.7}$$

We will use that in the t-channel the relation between $(Z,\overline{Z})$ and the cross-ratios $(z,\bar{z})$ is $(Z,\overline{Z}) = (1-z,1-\bar{z})$.

We now map the flat space to $\mathbb{R}\times S_R^{d-1}$ using

$$z = 1-Z = e^{-\frac{\tau}{R}-i\frac{x}{R}}\,, \qquad \bar{z} = 1-\overline{Z} = e^{-\frac{\tau}{R}+i\frac{\vec{x}}{R}}\,, \tag{A.8}$$

where R is the sphere radius and $\vec{x}$ schematically denotes all coordinates besides τ. This transformation introduces an overall prefactor in conformal partial waves

$$W_{\Delta',J'} = R^{-2\Delta}(z\bar{z})^{\frac{\Delta}{2}}\widehat{W}_{\Delta',J'} = R^{-2\Delta}\Big((1-Z)(1-\overline{Z})\Big)^{\frac{\Delta}{2}}\widehat{W}_{\Delta',J'}\,. \tag{A.9}$$

[31] Compared to [61] we omit the factor $(-2)^{-J}$ in the conformal waves.

JHEP10(2024)105

The $W_{\Delta',J'}$ are the CPW on $\mathbb{R}\times S^{d-1}_R$, where the two light operators are inserted at 0 and $(\tau,\vec{x})$ while the heavy operators sit at $-\infty$ and $+\infty$. Via the operator-state correspondence, the correlator on $\mathbb{R}\times S^{d-1}_R$ can be seen as a two-point function in a heavy state $\langle\mathcal{O}_H|\phi(\tau,x)\phi(0,0)|\mathcal{O}_H\rangle$.

Let us now focus on the exchanges of n-stress tensors, which have conformal dimension $\Delta'=d\,n$ and spin $J'=0,2,4,\ldots,2n$. Since these thermalize in heavy states [63], their expansion in CPW (A.9) precisely matches the corresponding expansion in terms of thermal conformal blocks [47]. We are interested in the OPE limit[32] $z,\bar{z}\to 1$ (or equivalently $Z,\overline{Z}\to 0$), which in $\mathbb{R}\times S^{d-1}_R$ corresponds to $\tau,|\vec{x}|\ll R$.

First consider the case with $x=|\vec{x}|=0$. In the regime $\tau\ll R$, the corresponding CPWs simplify to

$$d=2 \qquad W_{2n,J'}\approx 2\tau^{-2\Delta}\left(\frac{\tau}{R}\right)^{2n} \tag{A.10}$$

$$d=4 \qquad W_{4n,J'}\approx (1+J')\tau^{-2\Delta}\left(\frac{\tau}{R}\right)^{4n} \tag{A.11}$$

$$d=6 \qquad W_{6n,J'}\approx \frac{1}{6}(2+J')(3+J')\tau^{-2\Delta}\left(\frac{\tau}{R}\right)^{6n}\,. \tag{A.12}$$

Each n-stress tensor exchange is multiplied by a factor of μ^n, where[33]

$$\mu\propto\frac{\Delta_H}{C_T}\propto\varepsilon\frac{R^d}{C_T}\propto\left(\frac{R}{\beta}\right)^d\,. \tag{A.13}$$

In the above, we used that the energy density ε is proportional to $C_T\,T^d$ [47, 49]. It is convenient to isolate these dimensionful factors in the OPE coefficients and define

$$c_{d\,n,J'}\equiv\lambda_{n,J'}\left(\frac{R}{\beta}\right)^{d\,n}\,, \tag{A.14}$$

as in this case all dependence on the sphere radius R completely cancels out in the stress-tensor sector of the thermal correlator[34]

$$d=2\quad G_T(\tau)=\frac{1}{\tau^{2\Delta}}\left(1+2\lambda_{1,2}\left(\frac{\tau}{\beta}\right)^2+\sum_{n=2}^{\infty}\left[\sum_{J'}2\lambda_{n,J'}\right]\left(\frac{\tau}{\beta}\right)^{2n}\right)\,, \tag{A.15}$$

$$d=4\quad G_T(\tau)=\frac{1}{\tau^{2\Delta}}\left(1+3\lambda_{1,2}\left(\frac{\tau}{\beta}\right)^4+\sum_{n=2}^{\infty}\left[\sum_{J'}\lambda_{n,J'}(1+J')\right]\left(\frac{\tau}{\beta}\right)^{4n}\right)\,, \tag{A.16}$$

$$d=6\quad G_T(\tau)=\frac{1}{\tau^{2\Delta}}\left(1+\frac{10}{3}\lambda_{1,2}\left(\frac{\tau}{\beta}\right)^6+\sum_{n=2}^{\infty}\left[\sum_{J'}\lambda_{n,J'}\frac{(2+J')(3+J')}{6}\right]\left(\frac{\tau}{\beta}\right)^{6n}\right)\,, \tag{A.17}$$

[32] In this limit we effectively work on $\mathbb{R}^d$. It is however important to distinguish this from the original flat space-time on which correlator (A.1) was formulated.

[33] In holographic theories, μ is also the mass parameter appearing in the metric of the AdS-Schwarzschild black hole, see for example (2.4). For a black brane in $d+1$ dimensions, the relation between μ and the (inverse) Hawking temperature is

$$\mu=\left(\frac{4\pi R}{d\,\beta}\right)^d\,,$$

which scales with R/β exactly as in (A.13).

[34] The subscript in $G_T(\tau)$ denotes that this is the stress-tensor sector and *not* the full correlator.

JHEP10(2024)105

where the sums over J' run over $J' = 0, 2, \ldots 2\,n$. Finally, it is useful to introduce summed coefficients Λ_n through

$$G_T(\tau) = \frac{1}{\tau^{2\Delta}} \sum_{n=0}^{\infty} \Lambda_n \left(\frac{\tau}{\beta}\right)^{d\,n} , \tag{A.18}$$

which we use in the main text.

Now let x be small, but non-vanishing, such that $x \ll \tau \ll R$. For concreteness, we focus only on $d = 4$. Mapping the flat space CPW (A.3) to $\mathbb{R} \times S_R^{d-1}$, taking the OPE limit, and then expanding in $x \ll \tau$, we get the stress-tensor sector of the correlator as

$$G_T(\tau, x) = \frac{1}{\tau^{2\Delta}} \left(1 - \frac{\Delta\, x^2}{\tau^2}\right) \sum_{n=0}^{\infty} \left[\Lambda_n + \left(2\,n\,\Lambda_n + \widetilde{\Lambda}_n^{(1)}\right) \frac{x^2}{\tau^2}\right] \left(\frac{\tau}{\beta}\right)^{4\,n} + \mathcal{O}\left(x^4\right), \tag{A.19}$$

with Λ_n defined in (A.18) and

$$\widetilde{\Lambda}_n^{(1)} = -\frac{1}{6} \sum_{J'=0,2,\ldots,2n} J'\,(1 + J')\,(2 + J')\,\lambda_{n,J'} \ . \tag{A.20}$$

Note that $n = 0$ corresponds to the identity contribution and thus $\widetilde{\Lambda}_0^{(1)} = 0$, while at $n = 1$ the only non-vanishing contribution comes from the stress tensor with $J' = 2$.

To make the notation for $x \neq 0$ more transparent, we generalise equation (A.18) to

$$G_T(\tau, x) = \frac{1}{\tau^{2\Delta}} \sum_{n=0}^{\infty} \left[\Lambda_n^{(0)} + \frac{x^2}{\tau^2}\,\Lambda_n^{(1)} + \mathcal{O}\left(\frac{x^4}{\tau^4}\right)\right] \left(\frac{\tau}{\beta}\right)^{dn} , \tag{A.21}$$

where $\Lambda_n^{(0)} \equiv \Lambda_n$ and $\Lambda_n^{(1)} \equiv (2n - \Delta)\Lambda_n + \widetilde{\Lambda}_n^{(1)}$. In the same way one can define $\Lambda_n^{(m)}$ for any m. Note that the holographic method we used to determine the stress-tensor contributions extracts $\lambda_{n,J'}$ [24]. This means that in principle one can use this method to obtain the coefficients $\Lambda_n^{(m)}$ to arbitrary high orders in m and n.

Let us conclude this appendix by comparing the above analysis with the expansion of the correlator using the thermal conformal blocks formulated on $\mathbb{S}^1_\beta \times \mathbb{R}^{d-1}$ [47]

$$G_T(\tau, x) = \frac{1}{|\tau^2 + x^2|^{\Delta}} \sum_{n=0}^{\infty} \sum_{J'=0,2,\ldots,2n} \hat{\lambda}_{n,J'} \frac{|\tau^2 + x^2|^{\frac{dn}{2}}}{\beta^{dn}} C_{J'}^{\left(\frac{d+2}{2}\right)} \left(\frac{\tau}{\sqrt{\tau^2 + x^2}}\right) , \tag{A.22}$$

where $C_{J'}^{(\nu)}(\eta)$ are Gegenbauer polynomials and $\hat{\lambda}_{n,J'}$ are dimensionless coefficients. Imposing $x = 0$ and restricting to $d > 2$, (A.22) simplifies to

$$G_T(\tau) = \frac{1}{\tau^{2\Delta}} \sum_{n=0}^{\infty} \sum_{J'=0,2,\ldots,2n} \hat{\lambda}_{n,J'} \binom{d-3+J}{J} \left(\frac{\tau}{\beta}\right)^{dn} . \tag{A.23}$$

This can now be compared with the equations (A.16) and (A.17). For $d = 4$ one finds $\hat{\lambda}_{n,J'} = \lambda_{n,J'}$, while in $d = 6$ there is a conventional difference by a factor $(J + 1)$ in the coefficients $\lambda_{n,J'}$ and $\hat{\lambda}_{n,J'}$.

JHEP10(2024)105

B Bulk equation of motion

In this appendix we give the explicit form of the equation of motion

$$(\Box - m^2)\phi = 0\,, \qquad m^2 = \Delta(\Delta - d) \tag{B.1}$$

in the background of $(d+1)$-dimensional planar Euclidean Schwarzschild-AdS black hole after the coordinate transformation

$$\rho^2 = r^2\vec{x}^2 \quad \text{and} \quad w^2 = 1 + r^2(\tau^2 + \vec{x}^2). \tag{B.2}$$

Introducing the following ansatz for the scalar bulk field

$$\phi(w,\rho,r) = \left(\frac{r}{w^2}\right)^{\Delta} \psi(w,\rho,r)\,, \tag{B.3}$$

where $(r/w^2)^{\Delta}$ is the solution in the pure AdS space, "reduces" the Klein-Gordon equation (B.1) to [24]

$$\left(\partial_r^2 + C_1\partial_w^2 + C_2\partial_\rho^2 + C_3\partial_r\partial_w + C_4\partial_r\partial_\rho + C_5\partial_w\partial_\rho + C_6\partial_r + C_7\partial_w + C_8\partial_\rho + C_9\right)\psi = 0\,, \tag{B.4}$$

with the coefficients C_i given by

$$C_1 = \frac{f\left(\rho^2 + (w^2-1)^2 f\right) + w^2 - \rho^2 - 1}{r^2 w^2 f^2}\,, \tag{B.5}$$

$$C_2 = \frac{1 + f\rho^2}{r^2 f}\,, \tag{B.6}$$

$$C_3 = \frac{2}{rw}(w^2 - 1)\,, \tag{B.7}$$

$$C_4 = \frac{2\rho}{r}\,, \tag{B.8}$$

$$C_5 = \frac{2\rho}{r^2 w f}\left(1 + (w^2-1)f\right)\,, \tag{B.9}$$

$$C_6 = \frac{1}{f}\frac{\mathrm{d}f}{\mathrm{d}r} + \frac{w^2(10 - 4\Delta) + 8\Delta}{2rw^2} + \frac{d-4}{r}\,, \tag{B.10}$$

$$\begin{aligned} C_7 = {} & \left(\frac{1}{rwf}\frac{\mathrm{d}f}{\mathrm{d}r} - \frac{w^2(2\Delta - 5) - 4\Delta - 1}{r^2 w^3}\right)\left(w^2 - 1\right) \\ & + \frac{3w^2 - \rho^2(1 + 4\Delta)}{r^2 w^3 f} + \frac{1 + \rho^2 + 4\left(1 - w^2 + \rho^2\right)\Delta}{r^2 w^3 f^2} + (d-4)\frac{C_5}{2\rho}\,, \end{aligned} \tag{B.11}$$

$$C_8 = \frac{2(w^2 - 2\rho^2\Delta) + \rho^2\left(w^2(5 - 2\Delta) + 4\Delta\right) f}{r^2 w^2 \rho f} + \frac{\rho}{rf}\frac{\mathrm{d}f}{\mathrm{d}r} + (d-4)\frac{C_2}{\rho}\,, \tag{B.12}$$

$$\begin{aligned} C_9 = {} & \frac{\Delta}{w^2}\left(\frac{(w^2-2)^2\Delta + 4(1 + w^2 - w^4)}{r^2 w^2} + \frac{4\rho^2(\Delta + 1) - w^4(\Delta - 4) - 6w^2}{r^2 w^2 f}\right. \\ & \left. + \frac{2w^2(1 + 2\Delta) - 4(1 + \rho^2)(1 + \Delta)}{r^2 w^2 f^2} - \frac{w^2 - 2}{rf}\frac{\mathrm{d}f}{\mathrm{d}r} - (d-4)\frac{(w^2-2)(f-1)}{r^2 f}\right)\,, \end{aligned} \tag{B.13}$$

where $f = 1 - \frac{\mu}{r^d}$.

C Validity of approximating the OPE by an integral

In the main text we have approximated the OPE sums by an integral, such as in (3.16). In this appendix we now discuss the validity of this approximation.

We want to resum the OPE (3.9) where the coefficients are given by their asymptotic form (3.13). Assume that this asymptotic form is a good approximation to the actual OPE coefficients after a certain value $n = n_*$ and that one can neglect terms with $n < n_*$. The first assumption comes from our analysis of OPE data. We can justify the second assumption by noting that near the critical points $\tau \approx \tau_c$, which are at the radius of convergence of the stress-tensor OPE, all terms in the τ expansion contribute. One sees from (3.13) that for large enough Δ the OPE coefficients are increasing with n and thus close enough to the critical points, the large-n terms will be the most important. All in all, to calculate the stress-tensor contribution to the correlator, one has to evaluate a sum of the type

$$\sum_{n=n_*}^{\infty} n^{a\Delta+b} y^{dn} = y^{d\,n_*}\,\Phi\left(y^d, -a\Delta - b, n_*\right)\,, \tag{C.1}$$

where Φ is the Hurwitz-Lerch transcendent, $|y| \leq 1$, and $a > 0$ and b are constants. We want to compute this sum in the limit $y \to 1$, which corresponds to the correlator near $\tau \approx \tau_c$. For $\Delta > -\frac{a+b}{2}$, one can expand

$$\begin{aligned} &y^{d\,n_*}\,\Phi(y^d, -a\Delta - b, n_*) \\ &\qquad = \Gamma(1 + a\Delta + b)(-\log y^d)^{-(1+a\Delta+b)} + \sum_{k=0}^{\infty} \zeta(-a\Delta - b - k, n_*)\frac{\left(\log y^d\right)^k}{k!}\,, \end{aligned} \tag{C.2}$$

where ζ is the generalised Riemann zeta function. The second term is regular at $y = 1$ for all k, so it gives a subleading contribution to the correlator near the critical point. Therefore, near $\tau \approx \tau_c$ we can approximate the sum (C.1) by

$$\sum_{n=n_*}^{\infty} n^{a\Delta+b} y^{dn} \approx \Gamma(1 + a\Delta + b)(-\log y^d)^{-(1+a\Delta+b)} = \int_0^{\infty} n^{a\Delta+b} y^{dn}\, dn\,. \tag{C.3}$$

This justifies the exchange of the sum for an integral from 0 to ∞.

D The KMS pole and OPE in $d = 2$

In this appendix we show how the KMS pole emerges from the OPE in $d = 2$. The finite temperature two-point function is known in a closed form and the KMS pole can be seen explicitly without the use of the OPE. Nevertheless, the recovery of the KMS pole from the OPE can serve as a guideline for the analysis in higher dimensional cases, where the thermal two-point functions are not known exactly.

D.1 KMS pole

Consider a scalar two-point function at finite temperature $T = \beta^{-1}$

$$G(\tau, x) = \langle \phi(\tau, x)\phi(0, 0)\rangle_\beta\,. \tag{D.1}$$

JHEP10(2024)105

This can be rewritten, using the periodicity of the trace, as

$$G(\tau,x)=\frac{1}{Z}\operatorname{Tr}e^{-\beta H}\phi(\tau,x)\phi(0,0)=\frac{1}{Z}\operatorname{Tr}e^{-\beta H}\phi(\beta,0)\phi(\tau,x)=G(\beta-\tau,-x)\,, \tag{D.2}$$

which is the KMS condition [43, 44]. Let us consider the case where $x=0$. For a unit-normalised scalar with scaling dimension Δ, the small τ behaviour is

$$G(\tau)\xrightarrow{\tau\to 0}\frac{1}{|\tau|^{2\Delta}}\,. \tag{D.3}$$

From (D.2), it then follows that G also has a *KMS pole* at

$$G(\tau)\xrightarrow{\tau\to\beta}\frac{1}{|\beta-\tau|^{2\Delta}}\,. \tag{D.4}$$

This analysis is valid for any quantum field theory at finite temperature. When dealing with CFTs one has the additional tool of the OPE with a non-vanishing radius of convergence, which is typically determined by the first singular point encountered in the complex plane. Thus, if there are no singularities closer to the origin, the KMS pole should be encoded in the asymptotic behaviour of the OPE.

D.2 OPE analysis

Let us consider a CFT in two dimensions. Since $S_\beta\times\mathbb{R}$ is conformally equivalent to $\mathbb{R}^2$, the two-point correlation function is known in a closed form [47], and in the case of two identical scalar operators it is given by

$$G(\tau,x)=\left[\frac{\beta}{\pi}\sinh\left(\frac{\pi(x-i\tau)}{\beta}\right)\right]^{-\Delta}\left[\frac{\beta}{\pi}\sinh\left(\frac{\pi(x+i\tau)}{\beta}\right)\right]^{-\Delta}\,, \tag{D.5}$$

where we have chosen the normalisation such that in the zero-temperature limit we recover unit norm, i.e. $\lim_{\beta\to\infty}G(\tau,x)=(\tau^2+x^2)^{-\Delta}$.

Let us first set $x=0$. In a two-dimensional CFT, only the Virasoro vacuum module contributes to the thermal correlator. In other words, the only non-zero contribution comes from the multi-stress tensors and thus the full correlator can be expanded as

$$G(\tau)=\frac{1}{\tau^{2\Delta}}\sum_n\Lambda_n\left(\frac{\tau}{\beta}\right)^{2n}\,. \tag{D.6}$$

The coefficients Λ_n can simply be read off from the expansion of the correlator (D.5) near $\tau=0$. We are interested in the behaviour of the OPE near its convergence radius, where we expect all terms in the expansion to be of similar magnitude. As such, we are interested in the behaviour of Λ_n for large values of n. One finds that for large enough n these can be written in a $1/n$ expansion (see figure 12)

$$\Lambda_n=\frac{2^{2\Delta}}{\Gamma(2\Delta)}n^{2\Delta-1}\sum_{k=0}^{\infty}\frac{c_k(\Delta)}{n^k}=\frac{2^{2\Delta}}{\Gamma(2\Delta)}n^{2\Delta-1}\left(1+\frac{c_1(\Delta)}{n}+\dots\right)\,, \tag{D.7}$$

JHEP10(2024)105

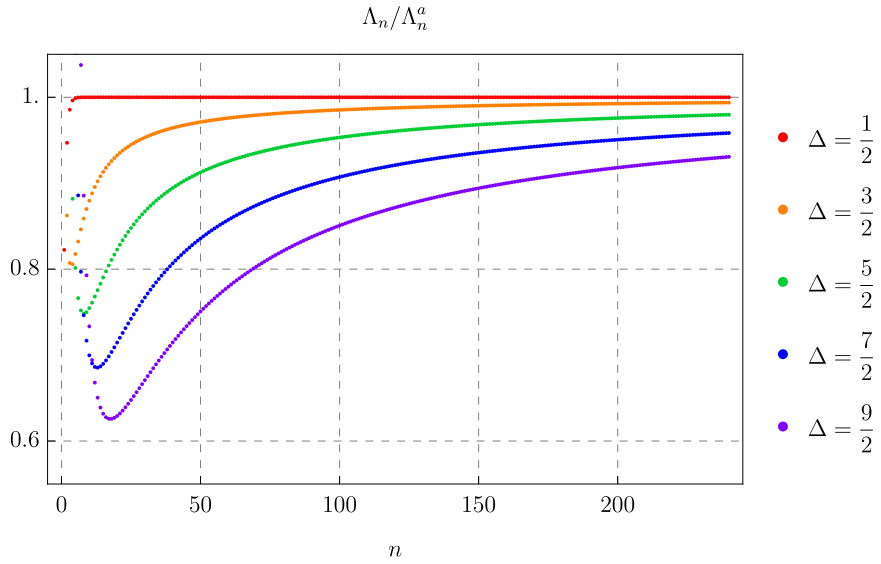

Figure 12. Ratio of the explicit results for Λ_n to the leading large-n prediction Λ_n^a, given in (D.8), for different values of Δ in $d = 2$.

where we choose the overall prefactor in such a way that $c_0(\Delta) = 1$, while all remaining $c_k(\Delta)$ can be arbitrary functions of Δ. We see that as $n \to \infty$ the coefficients tend to

$$\Lambda_n^a = \frac{2^{2\Delta}}{\Gamma(2\Delta)}\, n^{2\Delta-1}\,, \tag{D.8}$$

which determines the leading order behaviour of the correlator. For τ near the radius of convergence of the OPE (D.6), we can approximate the sum by an integral

$$G(\tau) \approx \frac{1}{\tau^{2\Delta}} \int_0^\infty \Lambda_n^a \left(\frac{\tau}{\beta}\right)^{2n} dn = \left[-\frac{\tau}{2}\log\left(\frac{\tau^2}{\beta^2}\right)\right]^{-2\Delta}\,, \tag{D.9}$$

where we have taken (D.8) for the OPE coefficients. We encounter a singularity when the argument of the logarithm is equal to 1, which happens at $\tau = \pm\beta$ where we find

$$G(\tau) \xrightarrow{\tau\to\pm\beta} \frac{1}{|\beta-\tau|^{2\Delta}}\,, \tag{D.10}$$

which are exactly the KMS poles (D.4). This explicitly shows that the asymptotic OPE analysis reproduces the first non-trivial poles of the full correlator (D.5) in the complex-τ plane. However, as may be expected, the OPE analysis does not contain any information about the higher order poles at $|\tau| > \beta$.

Subleading analysis. The above analysis shows that KMS pole is already contained in Λ_n^a, the leading behaviour of the OPE coefficients at large n. Let us now analyse the $1/n$ corrections in (D.7). The coefficients $c_k(\Delta)$ are determined by carefully analysing Λ_n as a function of Δ,[35] see blue markers in figure 13.

[35]We discuss how to determine the form of (D.7) and the values $c_k(\Delta)$ from Λ_n in more detail in appendix E, where we analyse the correlator in $d = 4$.

JHEP10(2024)105

Alternatively, one can follow a different approach to obtain coefficients $c_k(\Delta)$: insert the full expansion (D.7) into the sum (D.6) and again approximate it with an integral

$$\begin{aligned} G(\tau) &= \frac{2^{2\Delta}}{\Gamma(2\Delta)\,\tau^{2\Delta}} \int_0^\infty n^{2\Delta-1} \left(\frac{\tau}{\beta}\right)^{2n} \left(1 + \frac{c_1(\Delta)}{n} + \frac{c_2(\Delta)}{n^2} + \dots\right) dn \\ &= \left[-\tau \log\left(\frac{|\tau|}{\beta}\right)\right]^{-2\Delta} \left[1 + \frac{2\,c_1(\Delta)}{2\Delta-1}\left(-\log\left(\frac{|\tau|}{\beta}\right)\right)\right. \\ &\qquad \left. + \frac{4\,c_2(\Delta)}{(2\Delta-1)(2\Delta-2)}\left(-\log\left(\frac{|\tau|}{\beta}\right)^2\right) + \dots\right]. \end{aligned} \tag{D.11}$$

Expanding this result around[36] $\tau = \beta$ then gives

$$\begin{aligned} G(\tau) \xrightarrow{\tau\to\beta} \frac{1}{(\beta-\tau)^{2\Delta}} &\left[1 + \frac{1}{\beta}\left(\Delta + \frac{2\,c_1(\Delta)}{2\Delta-1}\right)(\beta-\tau)\right. \\ &\left. + \frac{1}{\beta^2}\left(\frac{\Delta(6\Delta+7)}{12} + \frac{(2\Delta+1)c_1(\Delta)}{2\Delta-1} + \frac{2\,c_2(\Delta)}{(2\Delta-1)(\Delta-1)}\right)(\beta-\tau)^2 + \dots\right]. \end{aligned} \tag{D.12}$$

We thus see that the $1/n$ corrections in (D.7) translate to $(\beta-\tau)$ corrections to the correlator near the KMS pole.

We can now use the exact form of the correlator (D.5) to determine the coefficients $c_k(\Delta)$. Expand (D.5) around $\tau = \beta$ to first subleading order

$$G(\tau) = \frac{1}{(\beta-\tau)^{2\Delta}}\left(1 + \frac{\Delta\,\pi^2}{3\,\beta^2}(\beta-\tau)^2 + \mathcal{O}\left((\beta-\tau)^3\right)\right). \tag{D.13}$$

This expression and (D.12) should match, which leads to

$$c_1(\Delta) = \Delta\left(\frac{1}{2} - \Delta\right), \qquad c_2(\Delta) = \frac{1}{24}\Delta\,(\Delta-1)(2\Delta-1)(6\Delta + 4\,\pi^2 - 1), \tag{D.14}$$

which can be continued to arbitrary k. One can compare these expressions with the direct data obtained from analysing the asymptotic form of Λ_n and find perfect agreement, see figure 13.

Nonzero x. Let us now set $x \neq 0$, so that $x \ll \tau$. Essentially, we work in the limit where x is the smallest length scale in the expression. Expanding the exact correlator (D.5) in small x gives to leading order

$$G(\tau, x) = \left[\frac{\beta}{\pi}\sin\left(\frac{\pi\,\tau}{\beta}\right)\right]^{-2\Delta} + \Delta\,x^2\left[\frac{\beta}{\pi}\sin\left(\frac{\pi\,\tau}{\beta}\right)\right]^{-2(\Delta+1)} + \mathcal{O}\left(x^4\right), \tag{D.15}$$

where each term contains non-trivial poles at $\tau = m\,\beta$, with $m \in \mathbb{Z}$. We expand each term in the above series individually around $\tau = \beta$, focusing only on the leading behaviour

$$G(\tau, x) \approx (\beta-\tau)^{-2\Delta}\left[1 + \frac{1}{(\beta-\tau)^2}\frac{\Delta\,x^2}{\beta^2}\right]. \tag{D.16}$$

[36] One can equally expand around $\tau = -\beta$, but we will focus on this pole without the loss of generality.

JHEP10(2024)105

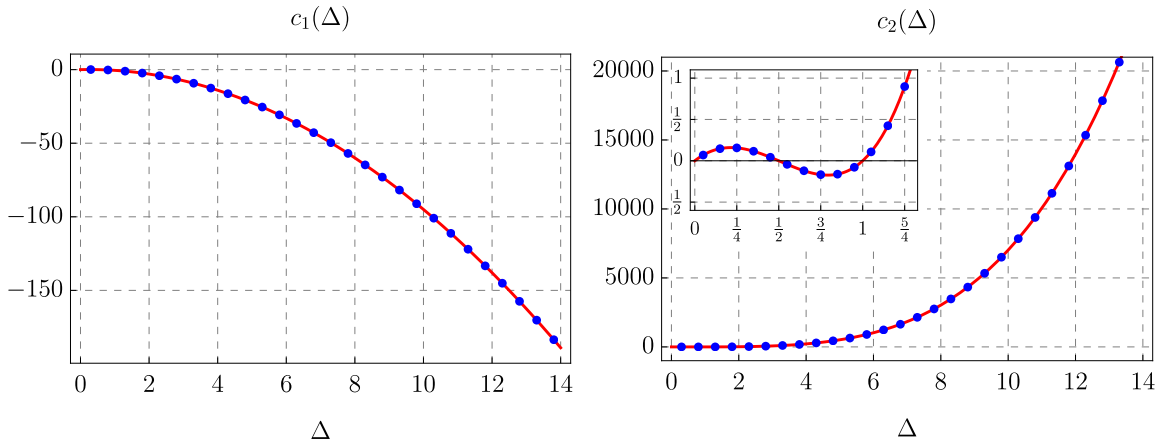

Figure 13. The comparison between $c_1(\Delta)$ (left) and $c_2(\Delta)$ (right) as obtained from expansion of the exact correlator (red curve) and the results from the direct analysis of Λ_n for large n (blue markers).

Naively, one would think that the x^2 term is more divergent than the leading order term. However, this expansion is only valid if x is the smallest parameter in the expression, i.e. $x^2 \ll (\beta-\tau)^2$, in which case all corrections to the leading divergent behaviour in (D.16) are small.

Similar to the analysis of the subleading $(\beta-\tau)$ contributions we would like to reproduce this result using the OPE analysis. For that we take (D.15) and expand each term individually in a series in τ

$$G(\tau,x)=\frac{1}{\tau^{2\Delta}}\left[\sum_{n=0}^{\infty}\Lambda_n^{(0)}\left(\frac{\tau}{\beta}\right)^{2n}+\frac{\Delta\,x^2}{\beta^2}\sum_{n=0}^{\infty}\Lambda_n^{(1)}\left(\frac{\tau}{\beta}\right)^{2n}+\mathcal{O}\left(x^4\right)\right]. \tag{D.17}$$

Again, we can make an ansatz for asymptotic behaviour of the OPE coefficients

$$\Lambda_n^{(\alpha)}=c_0^{(\alpha)}(\Delta)\,n^{a\,\Delta+b}, \tag{D.18}$$

where we ignore all $1/n$ corrections, since we are only interested in the leading behaviour at each order in x. We find

$$\Lambda_n^{(0)}\approx\frac{2^{2\Delta}}{\Gamma(2\Delta)}\,n^{2\Delta-1}, \qquad \Lambda_n^{(1)}\approx\frac{2^{2(\Delta+1)}}{\Gamma(2(\Delta+1))}\,n^{2\Delta+1}. \tag{D.19}$$

Inserting these values into (D.17) and replacing the sum with the integral leads to

$$\begin{aligned}G(\tau,x)&\approx\frac{1}{\tau^{2\Delta}}\int_0^{\infty}\left[\frac{2^{2\Delta}}{\Gamma(2\Delta)}\,n^{2\Delta-1}+\frac{\Delta\,x^2}{\beta^2}\,\frac{2^{2(\Delta+1)}}{\Gamma(2(\Delta+1))}\,n^{2\Delta+1}\right]\left(\frac{\tau}{\beta}\right)^{2n}dn\\&=\frac{1}{\tau^{2\Delta}}\left[\left(-\log\frac{|\tau|}{\beta}\right)^{-2\Delta}+\frac{\Delta\,x^2}{\beta^2}\left(-\log\frac{|\tau|}{\beta}\right)^{-2(\Delta+1)}\right].\end{aligned} \tag{D.20}$$

By expanding this near $\tau=\beta$ we exactly reproduce (D.16) — the asymptotic OPE analysis reproduces the KMS poles of the exact two-point correlation function for $x\neq 0$.

Let us conclude this appendix by noting that in the main text and in the appendices that follow we repeat this analysis for thermal correlators in higher dimensions. In these cases we

JHEP10(2024)105

can still extract $c_k(\Delta)$ (respectively $\Lambda_n^{(1)}$) by careful analysis of the OPE coefficients. However, since a closed form expression of the thermal correlator is not known, to cross-check these results we compare them with the geodesic analysis at subleading $\delta\tau$ (respectively $x \neq 0$).

E Analysis at subleading $\delta\tau$ in $d = 4$

In this appendix we analyse the contributions to $\mathcal{L}_T(\tau)$ subleading in $\delta\tau$ and how these arise as $1/n$ corrections to the asymptotic form of the OPE coefficients. This analysis is valid for any finite Δ. When $\Delta \to \infty$ the situation becomes more subtle. As we argued in section 3.4, in this limit, the cross-over point also goes to infinity, $n^* = \Delta/2 \to \infty$, which leads to disappearance of the bouncing singularity in $\mathcal{L}_T(\tau)$. However, as we saw in (3.21), taking Δ large *after* expanding the logarithm of the correlator near the bouncing singularity leads to the behaviour expected from the bouncing geodesic. Below we examine if this match persists beyond the leading order singularity. We also detail the procedure that we used in the main text to determine the asymptotic form of the OPE coefficients Λ_n.

The main object of interest are the OPE coefficients Λ_n, as defined in (3.9). In particular, we are interested in their behaviour when n is large. Ideally, one would find the exact expressions of these OPE coefficients as functions of Δ, however, in practice, finding such expressions for large n is computationally too expensive. As already mentioned in the main part of this paper, it is more efficient to first fix Δ and then calculate Λ_n for that specific value. In this way, we are able to calculate Λ_n up to $n \approx 50$ in about 5 days on a standard desktop machine.

We find that for large enough n the OPE coefficients can be described by

$$\Lambda_n = c(\Delta) \frac{n^{2\Delta-3}}{\left(\frac{1}{\sqrt{2}}\right)^{4n} e^{i\pi\, n}} \sum_{k=0}^{\infty} \frac{c_k(\Delta)}{n^k}\,, \tag{E.1}$$

where we choose $c_0(\Delta) = 1$, so that this expression is in accord with the dominant contribution (3.13) used in the main text. Let us here briefly explain how we obtained this expression. First, one draws inspiration from the two-dimensional analysis (D.7) and considers an ansatz for the dominant contribution $\Lambda_n^a = e^{-i\pi\, n} \widetilde{k}^n\, c(\Delta) n^{a\,\Delta+b}$. The first factor comes from the observed oscillating sign of Λ_n, while $\widetilde{k}$, a, and b are constants and $c(\Delta)$ is a function which all need to be determined by our analysis. The values of the three constants can be determined by analysing different ratios of Λ_n as n and Δ are varied. The expressions for $c(\Delta)$ and $c_k(\Delta)$ are then obtained numerically by analysing Λ_n as n is varied for fixed values of Δ. One first assumes the $1/n$ expansion (E.1) and compares it with the values of Λ_n as a function of n. This allows us to read off the coefficients $c_k(\Delta)$. This procedure gives, for example, the values given in the blue markers in figure 7, figure 14, and figure 15.

Let us note that the accuracy of our analysis is limited by the number of Λ_n we can calculate: the larger the n, the more accurate the asymptotic form (E.1) will be. A higher n also means that we can include, in practice, a higher number of $1/n$ corrections, which in turn allow for a more accurate values of $c_k(\Delta)$. An estimate of the value of n necessary for an accurate determination of Λ_n for a given Δ is given at the end of this appendix.

JHEP10(2024)105

The $1/n$ terms in (E.1) are mapped to the $(\tau_c - \tau)$ corrections of the correlator. To see this, we insert the full $1/n$ expansion of Λ_n into (3.9) and replace the sum with an integral

$$G_T(\tau) \approx \frac{1}{\tau^{2\Delta}} \int_0^\infty \Lambda_n \left(\frac{\tau}{\beta}\right)^{4n} dn = \frac{c(\Delta)}{\tau^{2\Delta}} \int_0^\infty n^{2\Delta-3} \left(\frac{\tau}{\tau_c}\right)^{4n} \sum_{k=0}^{\infty} \frac{c_k(\Delta)}{n^k}\, dn$$
$$= \frac{c(\Delta)}{\tau^{2\Delta}} \sum_{k=0}^{\infty} c_k(\Delta)\, \Gamma(2\Delta - 2 - k) \left[-\log\left(\frac{\tau^4}{\tau_c^4}\right)\right]^{-(2\Delta-2-k)}, \tag{E.2}$$

where τ_c is schematically one of the critical points defined in (3.17). We see that near $\tau \approx \tau_c$ we get a sum of diverging terms with a pole of order $2\Delta - 2 - k$: the higher the k, the milder the singularity.

In four dimensions, we lack an exact expression for the correlator (or the stress-tensor sector of the correlator), so we cannot determine $c_k(\Delta)$ in a similar manner as in the two-dimensional case. However, we can take the large-Δ limit and compare these results with the expectation from the geodesic analysis. In particular, we know that the correlator obtained from the bouncing geodesic expanded around the lightcone singularity receives the first correction to the leading result at fourth order (2.28). Therefore, we insert (E.2) into (3.19) and expand in $\delta\tau = \tau_c - \tau$

$$\mathcal{L}_T \approx -\frac{1}{\Delta} \log\left[\frac{c(\Delta)\,\Gamma(2\Delta-2)}{4^{(2\Delta-2)}} \frac{1}{\tau_c^2}\right] + \frac{2\Delta-2}{\Delta} \log \delta\tau + \sum_{k=1}^{\infty} \gamma_k(\Delta) \left(\frac{\delta\tau}{\tau_c}\right)^k, \tag{E.3}$$

where $\gamma_k(\Delta)$ are non-trivial combinations of $c_k(\Delta)$. Let us check if the $\Delta \to \infty$ limit reproduces the geodesic result (2.27), which means that

$$\gamma_1(\Delta) = 0\,, \qquad \gamma_2(\Delta) = 0\,, \qquad \gamma_3(\Delta) = 0\,, \qquad \gamma_4(\Delta) = \frac{\pi^4}{160}\,, \quad \dots\,, \tag{E.4}$$

up to $1/\Delta$ corrections. We only focus on $\gamma_1(\Delta)$ and $\gamma_2(\Delta)$. The former is given by

$$\gamma_1(\Delta) = 1 + \frac{1}{\Delta} + \frac{4\,c_1(\Delta)}{\Delta(2\Delta-3)}\,, \tag{E.5}$$

which can be expanded in large-Δ to first few orders

$$\gamma_1(\Delta) = 1 + \frac{1}{\Delta} + \frac{2\,c_1(\Delta)}{\Delta^2} + \frac{3\,c_1(\Delta)}{\Delta^3} + \mathcal{O}\left(\Delta^{-4}\right). \tag{E.6}$$

For this expression to be consistent with the bouncing geodesic, the leading behaviour of $c_1(\Delta)$ has to be given by

$$c_1(\Delta) \sim -\frac{\Delta^2}{2} + \dots\,, \tag{E.7}$$

which cancels out the leading order term in (E.6). However, we can be slightly bolder and assume that $\gamma_1(\Delta) = 0$ for all Δ, which ensures absence of a linear term in the proper length and the correlator. In this case, we can solve (E.5) directly and find

$$c_1(\Delta) = -\frac{1}{4}(\Delta+1)(2\Delta-3)\,, \tag{E.8}$$

JHEP10(2024)105

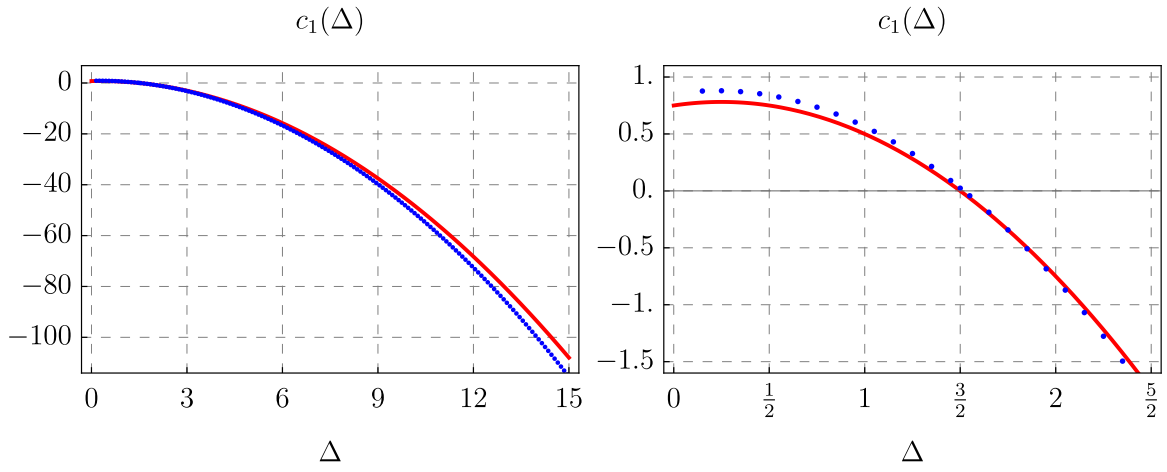

Figure 14. The numerical values for $c_1(\Delta)$ (blue) compared with the data predicted by the geodesic analysis (red). On the right, the close-up shows that even at small Δ the geodesic results seems to match the data to a relatively high degree. This suggests that even in the full correlator, there is no term linear in $\delta\tau = \tau_c - \tau$.

whose large Δ behaviour agrees with (E.7). In figure 14, we plot the numerical data (in blue) against this prediction (in red). We find good agreement not only at large Δ, but for all values which strongly suggests that $c_1(\Delta)$ is given by (E.8). The expression for $\gamma_2(\Delta)$ is more complicated

$$\gamma_2(\Delta) = -\frac{7}{12} - \frac{5}{12\,\Delta} - \frac{2\,c_1(\Delta)}{\Delta(2\Delta-3)} + \frac{8\,c_1(\Delta)^2}{\Delta(2\Delta-3)^2} - \frac{8\,c_2(\Delta)}{\Delta(6-7\Delta+2\Delta^2)} \tag{E.9a}$$

$$\approx -\frac{7}{12} - \frac{5}{12\,\Delta} - \frac{c_1(\Delta)}{\Delta^2} - \frac{4\,c_2(\Delta) - 2c_1(\Delta)^2 + \frac{3}{2}\,c_1(\Delta)}{\Delta^3} + \mathcal{O}\left(\Delta^{-4}\right). \tag{E.9b}$$

Above we have not yet inserted the value of $c_1(\Delta)$ because it will help us illustrate an important point as to why higher $c_k(\Delta)$ are inaccessible. As seen in (E.7), even in the most agnostic estimate $c_1(\Delta)$ scales at most quadratically at large values of Δ. Therefore, the $c_1(\Delta)^2$ factor in the fourth term will contribute at order Δ in (E.9b).[37] Such term is incompatible with a smooth large-Δ limit, independent of whether the geodesic is the bouncing geodesic or a non-singular complex geodesic. It therefore needs to be cancelled by the leading order term in $c_2(\Delta)$, which in this case gives

$$c_2(\Delta) \sim \frac{\Delta^4}{8} + \dots . \tag{E.10}$$

It needs to be stressed that this behaviour does not contain any information about whether the correlator is given by the bouncing geodesics or by the combination of two complex geodesics. This is contained in the subleading behaviour of $c_2(\Delta)$, which can be determined uniquely only if one knows the subleading behaviour of $c_1(\Delta)$. To illustrate this, let us

[37] We see from (E.9a) that $c_1(\Delta)$ appears at most quadratically in γ_2 and thus no higher order term in the $1/\Delta$ expansion will contribute at order Δ when the value of $c_1(\Delta)$ is inserted.

JHEP10(2024)105

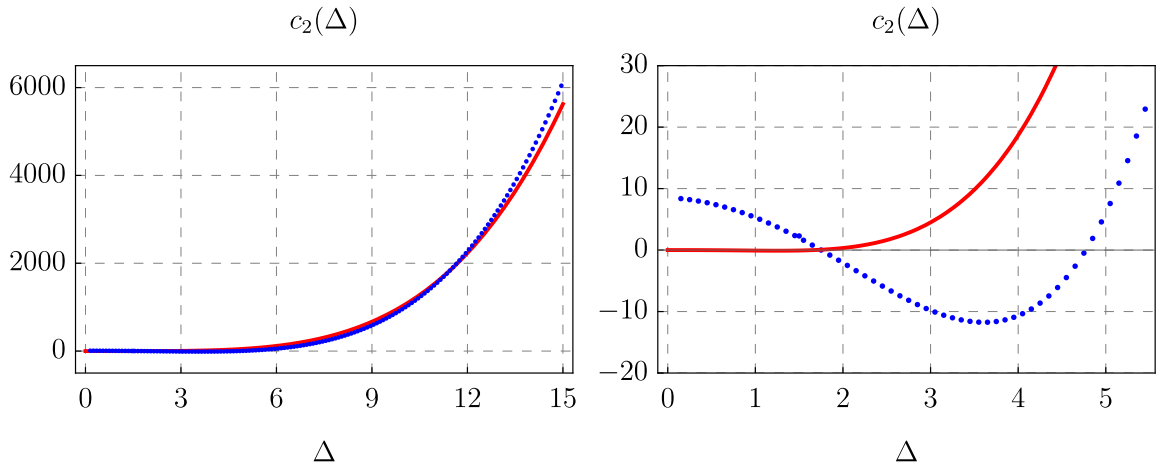

Figure 15. The numerical values for $c_2(\Delta)$ (blue) compared with the data predicted by the geodesic analysis (red). On the right, the close-up shows that at small Δ the geodesic prediction disagrees with the numerical data. This is expected, since there is no reason for the geodesic result to be applicable outside the regime where $\Delta \gg 1$.

introduce an expansion

$$c_1(\Delta) = c_1^{(2)}\,\Delta^2 + c_1^{(1)}\,\Delta + c_1^{(0)} + \dots\,, \quad c_2(\Delta) = c_2^{(4)}\,\Delta^4 + c_2^{(3)}\,\Delta^3 + c_2^{(2)}\,\Delta^2 + \dots\,, \tag{E.11}$$

and insert it into (E.9b)

$$\begin{aligned}\gamma_2(\Delta) = 2\Delta\left[\left(c_1^{(2)}\right)^2 - 2\,c_2^{(4)}\right] \\ + \frac{1}{12}\left[-7 - 12\,c_1^{(2)} + 48\,c_1^{(1)}\,c_1^{(2)} + 72\left(c_1^{(2)} - 48c_2^{(3)} - 168c_2^{(4)}\right)^2\right] + \mathcal{O}\left(\frac{1}{\Delta}\right).\end{aligned} \tag{E.12}$$

The term that scales with Δ can be determined as explained above. But the term that does not scale with Δ, and gives a finite contribution in the large-Δ limit, depends on the subleading terms of both $c_1(\Delta)$ and $c_2(\Delta)$. Since we believe that $c_1(\Delta)$ can be determined exactly (E.8), one can determine $c_2^{(3)}$ and write

$$c_2(\Delta) = \frac{\Delta^4}{8} - \frac{5\,\Delta^3}{24} + \mathcal{O}\left(\Delta^2\right), \tag{E.13}$$

but other, lower order terms are out of reach, since they are not constrained by the geodesic result. We can compare this result with the data obtained from solving the bulk equations of motion, which is pictured in figure 15. We see that while the asymptotic behaviours match, we cannot say anything about the behaviour of $c_2(\Delta)$ for small values of Δ. In fact, one can directly solve (E.9a) and determine $c_2(\Delta)$ using (E.8) in the process. Even in this case one find significant deviation from the data obtained from the holographic calculation.

Of course, the geodesic analysis is expected to hold only at large values of the conformal dimensions. We observed this already in section 3.2, where the geodesic analysis failed to reproduce all $1/\Delta$ corrections at higher orders of the $\tau = 0$ OPE. However, $c_1(\Delta)$ predicted from the analysis of the bouncing geodesic is in good agreement with the holographic data

JHEP10(2024)105

for all values of Δ. This suggests that the linear correction to the singularity, $\gamma_1(\Delta)$, vanishes for all conformal dimensions and not just in the large-Δ limit. This is generically not true for all other $\gamma_k(\Delta)$, starting with $\gamma_2(\Delta)$, and suggest that for finite values of Δ, the contribution to the correlator from the stress-tensor sector near the bouncing singularity goes as

$$G_T(\tau \approx \tau_c) \sim \frac{c(\Delta)\,\Gamma(2\Delta-2)}{2^{2(2\Delta-2)}}\,\frac{1}{\tau_c^2}\,\frac{1}{(\tau_c-\tau)^{2\Delta-2}}\left[1+\gamma_2(\Delta)\left(\frac{\tau_c-\tau}{\tau_c}\right)^2+\dots\right], \tag{E.14}$$

where $\gamma_2(\Delta)$ is some non-trivial function of Δ.

Higher order $c_k(\Delta)$ cannot be uniquely determined because we are unable to determine $c_2(\Delta)$ to all orders — the reasoning is the same as with the subleading order in $c_2(\Delta)$ only being accessible if we know $c_1(\Delta)$ to subleading order. One is only able to determine that the leading behaviour at large Δ is

$$c_k(\Delta) \sim \frac{(-1)^k\,\Delta^{2k}}{2^k\,k!}\,. \tag{E.15}$$

One can show that this behaviour is compatible with the holographic data obtained from solving the bulk equations of motion. However, as already discussed above, (E.15) does not contain any information about the specific geodesic that contributes to the correlator — this information is encoded in the subleading terms which we are unable to access with out current precision.

The large-Δ behaviour (E.15) serves as a useful rough estimate for the amount of terms in the $1/n$ expansion of Λ_n that give a considerable contribution at a fixed value of Δ. Let us assume that we can determine the Λ_n coefficients up to some number $n_{\max}$. At this point, the $1/n$ terms in (E.1) scale roughly as $\Delta^2/n_{\max}$. For $n_{\max} \lesssim \Delta^2$ the apparent $1/n$ expansion will not look convergent, since successive terms in the expansion will increase. In other words, the analysis can only be trusted for $\Delta \lesssim \sqrt{n_{\max}}$. In practice, we are able to reach $n_{\max} \approx 50$, which would suggest that we can fully trust the results up to $\Delta \approx 7$. It would thus be important if the method of obtaining Λ_n could be optimised so that $n_{\max}$ would be increased.

The main conceptual goal of this appendix was to check whether taking the large-Δ limit of the stress-tensor sector *after* we expanded the correlator near the bouncing singularity reproduces the results predicted by the bouncing geodesic. In particular, we focused on the subleading behaviour in $\delta\tau$. While we found no obvious disagreement, we have also not found any conclusive evidence that confirms a relation. Therefore, a more thorough analysis is needed to establish a definite connection between these two results.

F Analysis at non-zero x in $d = 4$

In this appendix we consider thermal correlation functions of scalar operators where the operators are inserted at a finite spatial distance, $x \neq 0$. We begin by discussing spacelike geodesics connecting the two insertion points and the effect of non-zero spatial distance on the bouncing geodesics. We then perform the OPE analysis for the stress-tensor sector at $x \neq 0$, expand the logarithm of the correlator near the bouncing singularity and *then* take the large-Δ limit. We find that due to a slower convergence, even the leading correction to the bouncing singularity at non-vanishing x cannot be conclusively matched between

JHEP10(2024)105

the geodesic and stress-tensor OPE results. We conclude that a more detailed analysis is needed to make a definite statement.

F.1 Semi-classical analysis

In contrast to the main part of the text, we work here directly in the Lorentzian signature and consider spacelike geodesics in (2.3). Let us parameterise the geodesics as $(t(s), r(s), x(s))$, where $s \in \mathbb{R}$ is the affine parameter. We can introduce conserved charges

$$E \equiv r^2 f(r)\, \dot{t}\,, \qquad P_i \equiv r^2\, \dot{x}_i\,, \tag{F.1}$$

where the dot denotes the derivative with respect to the affine parameter, which reduce finding the geodesics to a one-dimensional problem. We refer to P_i as the momentum and E as the (imaginary) energy, though we will omit the imaginary adjective in this appendix. The signs in (F.1) are chosen in such a way that in Patch I of the complexified spacetime (figure 2) the time increases for $E > 0$. Finally, we use the isometry of $\mathbb{R}^3$ and rotate the spacetime such that only one component of the momentum is non-vanishing, for example $P_1 \equiv P$. Generalising to having all momenta non-trivial is straightforward.

Spacelike geodesics in (2.3) have to satisfy the local constraint

$$-r^2 f(r)\, \dot{t}^2 + \frac{\dot{r}^2}{r^2 f(r)} + r^2\, \dot{x}^2 = 1\,, \tag{F.2}$$

which can be rewritten, using the expressions for the conserved charges, as

$$\dot{r}^2 - r^2 f(r) \left(1 - \frac{P^2}{r^2}\right) = E^2\,. \tag{F.3}$$

This effectively reduces the problem to classical scattering of a point particle in the potential (see figure 16)

$$V(r) = -r^2 f(r) \left(1 - \frac{P^2}{r^2}\right)\,. \tag{F.4}$$

The nature of the geodesics depends on the values of the conserved charges, which can be seen from the turning point determined by the solution of $E^2 = V(r)$. When $P = 0$, the potential is monotonically decreasing and goes to positive infinity at $r \to 0$. As $E \to \pm\infty$, we get close to the singularity — these are the bouncing geodesics discussed in the main text and in [8, 9]. When $P \neq 0$, we have to distinguish between $P > 1$ and $P < 1$ regimes, as was already pointed out in [8]. For $P > 1$, there exist one real turning point, which is always outside the horizon. Such geodesics never probe the region near the singularity and will not be of interest in our analysis. For $P < 1$, we can see that the behaviour near the origin changes — the potential now reaches a maximal value inside the horizon before going to negative infinity. While this drastically alters the strict $|E| \to \infty$ limit, the behaviour does not change if we consider the regime where $P\,E \ll 1$. Namely, this regime is where we can think of spatial displacement x (which is, as we will show, linearly related to the

JHEP10(2024)105

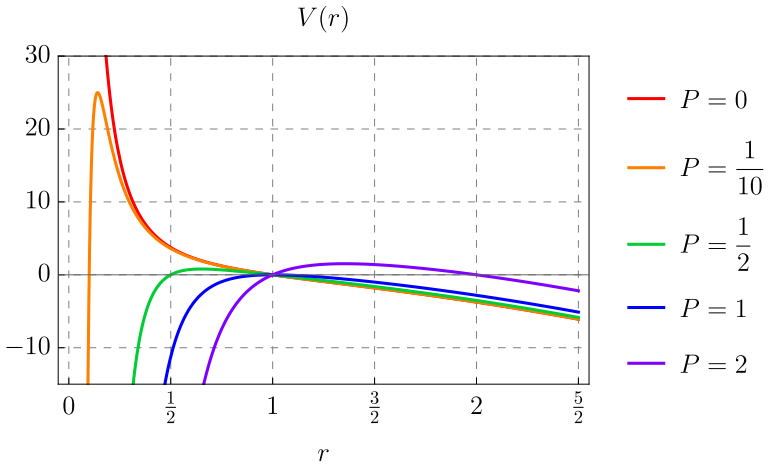

Figure 16. The potential $V(r)$ for different values of momentum P. When $P > 1$, the turning points are always outside the horizon and such geodesics do not probe the singularity. When $0 < P < 1$, the potential has a maximum inside the horizon. In our analysis, we consider the case where P (and thus x) is the smallest parameter of the problem and analyse perturbative corrections to the leading bouncing singularity due to non-vanishing spatial separation.

momentum P) as the smallest scale in the problem and treat it as an expansion parameter.[38] As such, we can compare the small x expansion on the geodesic side with the same expansion in the stress-tensor OPE (A.21) — in analogy of what was done in the two-dimensional example discussed in appendix D.

We want to calculate its regularised proper length and express it in terms of time and position displacements. The latter are given by

$$t \equiv t_f - t_i = 2\int_{r_t}^{\infty} \frac{E\, dr}{r^2 f(r)\sqrt{E^2 + r^2 f(r)\left(1 - \frac{P^2}{r^2}\right)}}\,, \tag{F.5a}$$

$$x = x_f - x_i = 2\int_{r_t}^{\infty} \frac{P\, dr}{r^2 \sqrt{E^2 + r^2 f(r)\left(1 - \frac{P^2}{r^2}\right)}}\,. \tag{F.5b}$$

whereas the proper length integral is

$$\mathcal{L} = 2\int_{r_t}^{r_{\max}} \frac{dr}{\sqrt{E^2 + r^2 f(r)\left(1 - \frac{P^2}{r^2}\right)}}\,. \tag{F.6}$$

In the above, r_t denotes the turning point of the geodesic, which is the largest real root of $E^2 = V(r)$, and we have used a cut-off parameter $r_{\max}$ that will help us to regularise the integral.

For $P \neq 0$ these integrals can be evaluated in terms of incomplete elliptic functions [46]. To express the solutions, we first define $q \equiv r^2$ and note that the turning point equation is

[38] Another justification as to why this is a valid expansion comes from the WKB analysis of the correlator [9]. There it was shown that the Fourier conjugate to the spatial distance x is actually $Q = -i\,P$. For purely imaginary momentum, the potential is monotonically decreasing as a function of r. In that case the behaviour of bouncing geodesics does not change as we increase x.

JHEP10(2024)105

a cubic equation in q. Let us denote the three, in general complex, solutions as q_1, q_2, and q_3, where q_1 corresponds to the largest real root and is identified with the turning point. Then one can show that the integrals (F.5) become

$$t = \frac{E}{\sqrt{q_1(q_3-q_2)}}\left[\frac{(q_3-q_1)}{(q_1-1)(q_3-1)}\Pi\left(\frac{c}{a},\phi,s\right)\right. \tag{F.7a}$$
$$\left. - \frac{(q_3-q_1)}{(q_1+1)(q_3+1)}\Pi\left(\frac{\bar{c}}{a},\phi,s\right) + \frac{2q_3^2}{(q_3-1)(q_3+1)}F\left(\phi,s\right)\right],$$
$$x = \frac{2\,P}{\sqrt{q_1\,(q_3-q_2)}}\,F(\phi,s)\,, \tag{F.7b}$$

where $F(\phi,s)$ and $\Pi(z,\phi,s)$ are incomplete elliptic integrals of the first and third kind respectively, and we have used

$$a = \frac{q_3-q_2}{q_1-q_2}\,, \qquad c = \frac{q_3-1}{q_1-1}\,, \qquad \bar{c} = \frac{q_3+1}{q_1+1}\,, \qquad s = \frac{q_3}{q_1\,a}\,, \qquad \phi = \arcsin\sqrt{a}\,. \tag{F.8}$$

Finally, the proper length integral is given by

$$\mathcal{L} = \lim_{r_{\rm max}\to\infty}\left\{2\sqrt{\frac{q_1}{q_3-q_2}}\left[s\,a\,F(\tilde{\phi},s) + (1-s\,a)\Pi\left(\frac{1}{a},\tilde{\phi},s\right)\right] - 2\,\log r_{\rm max}\right\}, \tag{F.9}$$

where

$$\tilde{\phi} \equiv \arcsin\left(\sqrt{a\frac{r_{\rm max}^2-q_1}{r_{\rm max}^2-q_3}}\right). \tag{F.10}$$

One can check that when $P=0$, these expressions reduce to (2.22).

We now use these expressions to calculate the leading x correction to the correlator near the bouncing singularity. Our method is to expand the expressions in P and take the $E\to\infty$ limit order by order. For example, at first order in P, the turning point (2.21) is given by

$$q_1 = \frac{1}{2}\left(\sqrt{4+E^4}-E^2\right) - P^2\,\frac{E^2}{\sqrt{4+E^2}}\,,+\mathcal{O}\left(P^4\right), \tag{F.11}$$

which, when taking $E\to\infty$ at each term separately, gives

$$q_1 = \frac{1}{E^2}\left[1-\varepsilon^2-\mathcal{O}\left(\varepsilon^4\right)\right]. \tag{F.12}$$

In the above, we have used

$$\varepsilon \equiv P\,E\,, \tag{F.13}$$

which is a convenient expansion parameter in this double limit, since this calculation only gives sensible results if x (or P in this instance) is the smallest parameter in the expansion. As such, $P \ll 1/E$ or equivalently $\varepsilon = P\,E \ll 1$, which is why this combination appears naturally in this limit.

One can then expand (F.7) in ε and express the conserved charges as

$$E = \frac{2}{\delta t}\,, \qquad \varepsilon = \frac{2}{\pi}\,\frac{x}{\delta t}\,, \tag{F.14}$$

JHEP10(2024)105

where $\delta t = -i\delta\tau = -t - i\tau_c$. The proper length integral expanded in ε is

$$\mathcal{L} \approx 2\log 2 - 2\log E + \frac{\pi}{2E^2}\,\varepsilon^2\,, \tag{F.15}$$

which, when expressed in terms of position space coordinates, gives

$$\mathcal{L} = 2\log(\delta t) + \frac{x^2}{2\pi}\,. \tag{F.16}$$

In a saddle point approximation, the contribution from such a geodesic to the correlator would be, to leading order in x

$$e^{-\Delta\,\mathcal{L}} \sim \frac{1}{(\delta t)^{2\Delta}}\left(1 - \frac{\Delta}{2\pi}\,x^2\right) = \frac{1}{(\delta t)^{2\Delta}}\left(1 - \frac{\Delta\,\pi}{2\,\beta^2}\,x^2\right)\,, \tag{F.17}$$

where in the last expression we reinstated the inverse temperature. This is the result that we will compare to the OPE analysis.

F.2 OPE analysis

Let us now discuss the CFT side of the $x \neq 0$ story. As discussed in appendix A, for $0 < x \ll \tau$ the decomposition of the correlator generalises to

$$G(\tau, x) = \frac{1}{\tau^{2\Delta}}\sum_{n=0}^{\infty}\left[\Lambda_n^{(0)} + \frac{x^2}{\tau^2}\Lambda_n^{(1)} + \mathcal{O}\left(\frac{x^4}{\tau^4}\right)\right]\left(\frac{\tau}{\beta}\right)^{4n}\,, \tag{F.18}$$

where $\Lambda_n^{(0)} \equiv \Lambda_n$ is the contribution at $x = 0$ that we examined in the main text. The coefficients $\Lambda^{(1)}$ can be further decomposed as

$$\Lambda_n^{(1)} \equiv (2n - \Delta)\,\Lambda_n + \widetilde{\Lambda}_n^{(1)}\,, \tag{F.19}$$

where $\widetilde{\Lambda}_n^{(1)}$ are given by (A.20) and can thus be determined using the same holographic calculation as $\Lambda_n^{(0)}$. Since the latter have already been analysed, we focus here on the asymptotic behaviour of $\widetilde{\Lambda}_n^{(1)}$. We find that this data is well described by

$$\widetilde{\Lambda}_n^{(1)} = c(\Delta)\,\frac{n^{2\Delta-2}}{\left(\frac{1}{\sqrt{2}}\right)^{4n} e^{i\pi\,n}}\sum_{k=0}^{\infty}\frac{d_k(\Delta)}{n^k}\,. \tag{F.20}$$

The most important difference compared to (3.13) is the power of the factor of n. As we will see, this has significant effects on the degree of the singularity at first non-trivial correction in x near the bouncing singularity. The prefactor $c(\Delta)$ is chosen to be the same as in $\Lambda_n^{(0)}$, in which case $d_0(\Delta)$ is not necessarily equal to 1. Let us note that the convergence of the numerical data obtained from solving the bulk equation of motion to (F.20) is slower compared to the convergence in the $x = 0$ case. We can trace this back to more prefactors in the expression for $\widetilde{\Lambda}_n^{(1)}$ (A.20) compared to $\Lambda_n^{(0)}$ (A.16). As such, the results in this appendix are less reliable. Nonetheless, one is able to extract some information even with $n \approx 50$ data points at each value of Δ.

JHEP10(2024)105

Combining (F.20) with the expansion for $\Lambda_n^{(0)}$ gives

$$\Lambda_n^{(1)} = c(\Delta)\,\frac{n^{2\Delta-2}}{\left(\frac{1}{\sqrt{2}}\,e^{\frac{i\pi}{4}}\right)^{4n}}\sum_{k=0}^{\infty}\frac{d_k(\Delta)+2\,c_k(\Delta)-\Delta\,c_{k-1}(\Delta)}{n^k}\,, \tag{F.21}$$

where we define $c_{-1}(\Delta)=0$. This, combined with the asymptotic form of $\Lambda_n^{(0)}$, can be inserted into the correlator expansion

$$\begin{aligned} G_T(\tau,x) &\approx \frac{c(\Delta)}{\tau^{2\Delta}}\int_0^\infty dn\left[n^{2\Delta-3}+\frac{x^2}{\tau^2}\,n^{2\Delta-2}\left(d_0(\Delta)+2+\frac{d_1(\Delta)+2c_1(\Delta)-\Delta}{n}\right)\right]\left(\frac{\tau^4}{\tau_c^4}\right)^n \\ &= \frac{c(\Delta)\,\Gamma(2\Delta-2)}{\tau^{2\Delta}}\left[-\log\left(\frac{\tau^4}{\tau_c^4}\right)\right]^{2-2\Delta} \\ &\quad\times\left\{1+\frac{x^2}{\tau^2}\left[\frac{(2\Delta-1)(d_0(\Delta)+2)}{-\log\left(\frac{\tau^4}{\tau_c^4}\right)}+d_1(\Delta)+2c_1(\Delta)-\Delta\right]\right\}, \end{aligned} \tag{F.22}$$

where we have again replaced the sum with an integral, inserted τ_c using (3.17), and used that $c_0(\Delta)=1$. In this expression we work only at leading order in n in the x^0 term while keeping the subleading contribution in the x^2 term. We will shortly show why the subleading correction is important. We can now expand the correlator around $\tau\approx\tau_c$, which gives the bouncing singularity together with several corrections

$$G(\tau,x)\approx\frac{c(\Delta)\,\Gamma(2\Delta-2)}{4^{2\Delta-2}}\,\frac{1}{\tau_c^2\,\delta\tau^{2\Delta-2}}\left[1+\frac{x^2}{\tau_c^2}\tilde{\gamma}_1(\Delta)+\frac{x^2}{\tau_c\,\delta\tau}\,\frac{(2\Delta-1)(2+d_0(\Delta))}{4}\right], \tag{F.23}$$

where we defined

$$\tilde{\gamma}_1(\Delta)\equiv d_1(\Delta)+\frac{-5+8\Delta+4\Delta^2}{8}\,d_0(\Delta)+2\,c_1(\Delta)-\frac{5}{4}+\Delta+\Delta^2\,. \tag{F.24}$$

To compare this analysis with the proper length of the bouncing geodesic we use (3.19) and take the large-Δ limit

$$\begin{aligned} \lim_{\Delta\to\infty}\mathcal{L}_T &= 2\log\delta\tau+\frac{x^2}{\tau_c^2}\left[\frac{3-2\Delta}{4\Delta}-\frac{d_1(\Delta)}{\Delta}-\frac{2c_1(\Delta)}{\Delta}-\frac{3(2\Delta-1)d_0(\Delta)}{8\Delta}\right] \\ &\quad+\frac{x^2}{\tau_c\,\delta\tau}\,\frac{(2\Delta-1)(2+d_0(\Delta))}{4\Delta}\,, \end{aligned} \tag{F.25}$$

where it should be understood that one needs to take $\Delta\to\infty$ in all terms in this expression. We immediately notice that in contrast to (F.16), the leading correction at x^2 comes at order $1/\delta\tau$. For the two expressions to be compatible, we would have to find

$$d_0(\Delta)=-2+\mathcal{O}\left(\frac{1}{\Delta}\right). \tag{F.26}$$

We compare this prediction with the numerical data coming from solving the bulk equations of motion in figure 17. We note that in the range $0\lesssim\Delta\lesssim 15$, the numerical data is roughly constant, but misses the value predicted by the geodesic analysis by about 10%.

JHEP10(2024)105

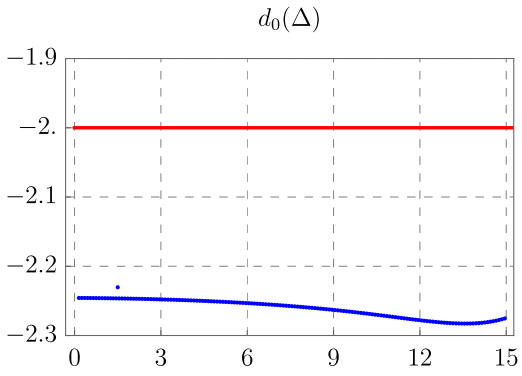

Figure 17. The geodesic prediction for $d_0(\Delta)$ (red) compared to the numerical data obtained using the holographic method (blue). We see that there is significant mismatch between the two results. We relate this to the slower convergence of the OPE data to the asymptotic form.

While we believe that this difference is due to the slow convergence of data toward the asymptotic OPE ansatz (F.20) and that when the number of OPE coefficients calculated is increased the numerical data will converge to the geodesic result, we currently cannot show that this is the case.

Since we cannot conclusively say something about the most divergent term at order x^2 in (F.25), we cannot compare the second term (with the square bracket) which has a counterpart in (F.16). However, we immediately run into an interesting problem: note that in the geodesic result, the first correction is real, while in the result from the OPE analysis, the analogous correction is multiplied by τ_c^2, which is imaginary. Not only that, this value differs based on which of the four poles was chosen to expand the correlator around. We currently do not have a good understanding of this discrepancy and leave this interesting avenue for future work. Let us also remark that from the CFT point of view having $x \neq 0$ does not significantly alter the physics, while the behaviour of the (real) bouncing geodesic changes [8] . It would be interesting to understand whether the difference in the prefactors is related to this phenomenon.

G Black hole singularity in $d = 6$ and $d = 8$

In this appendix we show that the stress-tensor sector in six and eight dimensional holographic CFTs also contains singularities at the critical values predicted by bouncing geodesics. In $d + 1$ spacetime dimensions the value of τ_c is given by [8]

$$\tau_c^{(d+1)} = \frac{\beta}{2} \pm i\frac{\beta}{2}\,\frac{\cos\frac{\pi}{d}}{\sin\frac{\pi}{d}} = \pm i\frac{\beta e^{\mp\frac{i\pi}{d}}}{2\sin\frac{\pi}{d}}\ . \tag{G.1}$$

Below we reproduce τ_c from the asymptotic analysis of the stress tensor OPE in $d = 6$ and $d = 8$.

JHEP10(2024)105

G.1 Singularity in six dimensions

We start by solving the 7-dimensional scalar equations of motion in the black-hole background using the ansatz (3.8). By expanding the results and comparing them with the CPW expansion (3.9), we extract the CFT data from the dual bulk theory. For example the first two OPE coefficients are

$$\Lambda_1 = \frac{8\pi^6\Delta}{15309} \tag{G.2}$$

$$\Lambda_2 = \frac{32\pi^{12}\Delta\left(715\Delta^5 - 6930\Delta^4 + 17204\Delta^3 - 9323\Delta^2 + 26334\Delta + 9000\right)}{167571318915(\Delta-6)(\Delta-5)(\Delta-4)(\Delta-3)}\,. \tag{G.3}$$

Again we are interested in the large-n behaviour of Λ_n. We find that as n grows, the OPE coefficients tend to

$$\Lambda_n^a = j(\Delta)n^{2\Delta-4}\,, \tag{G.4}$$

up to $1/n$ corrections which we do not here. In the above, $j(\Delta)$ is an undetermined function of the conformal dimension. An interesting difference compared to $d = 4$ is the absence of an oscillating sign in Λ_n^a. Inserting these coefficients into the OPE and approximating the sum with an integral gives

$$G_T(\tau) = \frac{1}{\tau^{2\Delta}}\int_0^\infty \Lambda_n^a\left(\frac{\tau}{\beta}\right)^{6n} dn = \frac{j(\Delta)\,\Gamma(2\Delta-3)}{\tau^{2\Delta}}\left(-\log\left(\frac{\tau^6}{\beta^6}\right)\right)^{3-2\Delta}\,. \tag{G.5}$$

This expression has a singularity whenever the argument of the logarithm is equal to 1, which is precisely at (see left panel of figure 18)

$$\tau_c = \beta e^{i\frac{k\pi}{3}} \quad \text{for} \quad k \in \mathbb{Z}\,. \tag{G.6}$$

Interestingly, we note that all singularities are located on a circle of radius β and that two of these critical points coincide with the positions where one expects KMS poles. When comparing these critical values to the geodesic result (G.1)

$$\tau_c^{(7)} = \frac{\beta}{2} \pm i\frac{\beta}{2}\sqrt{3} = \beta e^{\pm i\frac{\pi}{3}}\,, \tag{G.7}$$

we find a precise match.

G.2 Singularity in eight dimensions

We follow the same approach in $d = 8$. The first two coefficients are

$$\Lambda_1 = \frac{\pi^8\Delta}{184320} \tag{G.8}$$

$$\Lambda_2 = \frac{\pi^{16}\Delta}{1156266432921600(\Delta-8)(\Delta-7)(\Delta-6)(\Delta-5)(\Delta-4)} \times \left(17017\Delta^6 - 211666\Delta^5 + 681619\Delta^4 - 881554\Delta^3 + 3831472\Delta^2 + 2284352\Delta + 1317120\right)\,. \tag{G.9}$$

Overall we find that the leading asymptotic behaviour of the OPE coefficients is

$$\Lambda_n^a = Q(\Delta)\frac{n^{2\Delta-5}}{W^{8n}\,e^{i\pi\,n}}\,, \tag{G.10}$$

JHEP10(2024)105

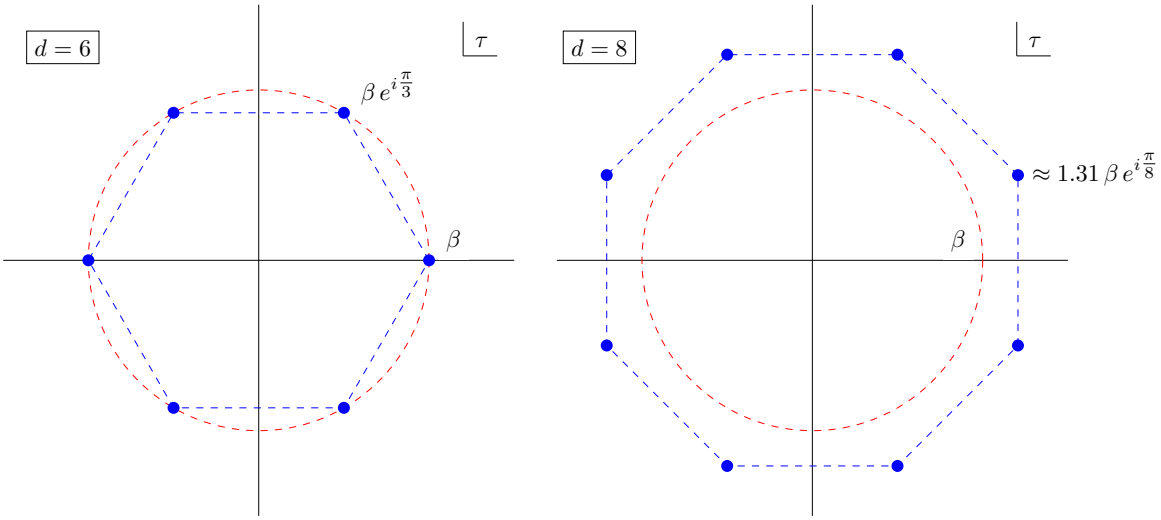

Figure 18. Poles in the complex τ plane in $d = 6$ and $d = 8$.

where $Q(\Delta)$ is a function of the conformal dimension and W is a constant

$$W \approx 1.3066 \ . \tag{G.11}$$

We note that the Λ_n^a have an oscillating sign, similar to the four-dimensional case. Inserting them in the OPE and performing the integral gives

$$G_T(\tau) = \frac{1}{\tau^{2\Delta}} \int_0^\infty \Lambda_n^a \left(\frac{\tau}{\beta}\right)^{8n} dn = \frac{Q(\Delta)\,\Gamma(2\Delta - 5)}{\tau^{2\Delta}} \left(-\log\left(\frac{\tau^8}{W\,\beta^8\, e^{i\pi}}\right)\right)^{3-2\Delta} . \tag{G.12}$$

I.e. the stress-tensor sector has a singularity at

$$\tau_c = \beta\, W\, e^{\frac{i\pi}{8} + k\frac{i\pi}{4}} \quad \text{for} \quad k \in \mathbb{Z}\,, \tag{G.13}$$

which are pictured on the right in figure 18. This agrees with the geodesic analysis which predicts the singularities at

$$\tau_c^{(9)} = \frac{\beta}{2} \pm i\frac{\beta}{2} \cot\frac{\pi}{8} = \beta \frac{e^{\pm i\frac{3\pi}{8}}}{2\sin\frac{\pi}{8}}\,, \tag{G.14}$$

since

$$\frac{1}{2\sin\frac{\pi}{8}} \approx 1.3066 \approx W \ . \tag{G.15}$$

It is interesting to note that in $d = 8$ these singularities are all located further away than where we would expect to find the KMS poles. This further strengthens the argument that the stress-tensor sector does not contain the information about the KMS poles and the double-traces are needed to recover their location.

H Lowest-twist analysis

In the main body of the paper we have examined the *summed coefficients* Λ_n defined by the expansion (A.18). It is also interesting to study the individual coefficients $\lambda_{n,J'}$ corresponding

JHEP10(2024)105

to the contributions from multi-stress tensors with different spin J' (respectively twist $\Delta'-J'$). We are mainly interested in the behaviour of the coefficients $\lambda_{n,2n}$ that correspond to the multi-stress tensors with the lowest twist. These coefficients are universal in holographic theories [24] and one can calculate them using bootstrap techniques (see e.g. [23]).

Alternatively, one can develop an effective method[39] to calculate $\lambda_{n,2n}$ by combining the bulk recursion relation found in [24], with the fact that only one coefficient of the bulk ansatz contributes to the near-lightcone correlator at each order in $1/r$ expansion.[40] Such coefficient can be then mapped to the lowest-twist coefficient $\lambda_{n,2n}$. In practice we get this coefficient as

$$\lambda_{n,2n} = \left(-\frac{\pi^4}{4}\right)^n b_{n,n} \,. \tag{H.1}$$

where $b_{n,n}$ can be systematically calculated by solving the recursion relation [24]:

$$4(j-4i)b_{i,j} = \frac{4(1-j+i)(i-j-1+\Delta)}{j-\Delta} b_{i,j-1} - 4(1+j-\Delta)b_{i-1,j+1} \tag{H.2}$$

where $i,j \in \mathbb{Z}$, $b_{i,j}=0$ for $j \notin [-i,i]$ and for all $i<0$, and $b_{0,0}=1$.

Analysing the coefficients $\lambda_{n,2n}$ we find their leading large-n behaviour to be

$$\lambda_{n,2n} = A(\Delta)\frac{e^{i\pi n} n^{2\Delta-5/2}}{B^{4n}} \,, \tag{H.3}$$

where $A(\Delta)$ is a function of the scaling dimension and value of the constant $B \approx 0.8968\ldots$.

To compare this with the asymptotic form of $\Lambda_n \sim n^{2\Delta-3}$, we consider the coefficient $\lambda_{n,2n}$ multiplied by $(1+J)$, yielding the behaviour $\sim n^{2\Delta-3/2}$ which grows faster than the overall summed coefficient Λ_n. Thus, terms with the subleading twists are crucial to ensure that Λ_n has the correct overall scaling as observed in the main part of the paper. It would be interesting to study this in more detail.

References

[1] J.M. Maldacena, *The large N limit of superconformal field theories and supergravity*, *Adv. Theor. Math. Phys.* **2** (1998) 231 [hep-th/9711200] [INSPIRE].

[2] S.S. Gubser, I.R. Klebanov and A.M. Polyakov, *Gauge theory correlators from noncritical string theory*, *Phys. Lett. B* **428** (1998) 105 [hep-th/9802109] [INSPIRE].

[3] E. Witten, *Anti-de Sitter space and holography*, *Adv. Theor. Math. Phys.* **2** (1998) 253 [hep-th/9802150] [INSPIRE].

[4] E. Witten, *Anti-de Sitter space, thermal phase transition, and confinement in gauge theories*, *Adv. Theor. Math. Phys.* **2** (1998) 505 [hep-th/9803131] [INSPIRE].

[39] This way one get access to the leading-twist OPE coefficients $\lambda_{n,2n}$ up to order $n \sim 10000$.

[40] This is an analogous approach as the one used in the appendix A of [35].

JHEP10(2024)105

[5] J.M. Maldacena, *Eternal black holes in anti-de Sitter*, *JHEP* **04** (2003) 021 [hep-th/0106112] [INSPIRE].

[6] J. Louko, D. Marolf and S.F. Ross, *On geodesic propagators and black hole holography*, *Phys. Rev. D* **62** (2000) 044041 [hep-th/0002111] [INSPIRE].

[7] P. Kraus, H. Ooguri and S. Shenker, *Inside the horizon with AdS/CFT*, *Phys. Rev. D* **67** (2003) 124022 [hep-th/0212277] [INSPIRE].

[8] L. Fidkowski, V. Hubeny, M. Kleban and S. Shenker, *The black hole singularity in AdS/CFT*, *JHEP* **02** (2004) 014 [hep-th/0306170] [INSPIRE].

[9] G. Festuccia and H. Liu, *Excursions beyond the horizon: black hole singularities in Yang-Mills theories. I*, *JHEP* **04** (2006) 044 [hep-th/0506202] [INSPIRE].

[10] G. Festuccia and H. Liu, *The arrow of time, black holes, and quantum mixing of large N Yang-Mills theories*, *JHEP* **12** (2007) 027 [hep-th/0611098] [INSPIRE].

[11] I. Amado and C. Hoyos-Badajoz, *AdS black holes as reflecting cavities*, *JHEP* **09** (2008) 118 [arXiv:0807.2337] [INSPIRE].

[12] T. Hartman and J. Maldacena, *Time evolution of entanglement entropy from black hole interiors*, *JHEP* **05** (2013) 014 [arXiv:1303.1080] [INSPIRE].

[13] H. Liu and S.J. Suh, *Entanglement Tsunami: universal scaling in holographic thermalization*, *Phys. Rev. Lett.* **112** (2014) 011601 [arXiv:1305.7244] [INSPIRE].

[14] H. Liu and S.J. Suh, *Entanglement growth during thermalization in holographic systems*, *Phys. Rev. D* **89** (2014) 066012 [arXiv:1311.1200] [INSPIRE].

[15] M. Grinberg and J. Maldacena, *Proper time to the black hole singularity from thermal one-point functions*, *JHEP* **03** (2021) 131 [arXiv:2011.01004] [INSPIRE].

[16] D. Rodriguez-Gomez and J.G. Russo, *Correlation functions in finite temperature CFT and black hole singularities*, *JHEP* **06** (2021) 048 [arXiv:2102.11891] [INSPIRE].

[17] S.A.W. Leutheusser and H. Liu, *Emergent times in holographic duality*, *Phys. Rev. D* **108** (2023) 086020 [arXiv:2112.12156] [INSPIRE].

[18] J. de Boer, D.L. Jafferis and L. Lamprou, *On black hole interior reconstruction, singularities and the emergence of time*, arXiv:2211.16512 [INSPIRE].

[19] J.R. David and S. Kumar, *Thermal one point functions, large d and interior geometry of black holes*, *JHEP* **03** (2023) 256 [arXiv:2212.07758] [INSPIRE].

[20] G.T. Horowitz, H. Leung, L. Queimada and Y. Zhao, *Boundary signature of singularity in the presence of a shock wave*, *SciPost Phys.* **16** (2024) 060 [arXiv:2310.03076] [INSPIRE].

[21] E. Parisini, K. Skenderis and B. Withers, *The ambient space formalism*, *JHEP* **05** (2024) 296 [arXiv:2312.03820] [INSPIRE].

[22] M. Dodelson et al., *Black hole bulk-cone singularities*, *JHEP* **07** (2024) 046 [arXiv:2310.15236] [INSPIRE].

[23] R. Karlsson, M. Kulaxizi, A. Parnachev and P. Tadić, *Leading multi-stress tensors and conformal bootstrap*, *JHEP* **01** (2020) 076 [arXiv:1909.05775] [INSPIRE].

[24] A.L. Fitzpatrick and K.-W. Huang, *Universal lowest-twist in CFTs from holography*, *JHEP* **08** (2019) 138 [arXiv:1903.05306] [INSPIRE].

[25] Y.-Z. Li, Z.-F. Mai and H. Lü, *Holographic OPE coefficients from AdS black holes with matters*, *JHEP* **09** (2019) 001 [arXiv:1905.09302] [INSPIRE].

JHEP10(2024)105

[26] A.L. Fitzpatrick et al., *Model-dependence of minimal-twist OPEs in $d > 2$ holographic CFTs*, *JHEP* **11** (2020) 060 [arXiv:2007.07382] [INSPIRE].

[27] R. Karlsson, A. Parnachev, V. Prilepina and S. Valach, *Thermal stress tensor correlators, OPE and holography*, *JHEP* **09** (2022) 234 [arXiv:2206.05544] [INSPIRE].

[28] K.-W. Huang, R. Karlsson, A. Parnachev and S. Valach, *Freedom near lightcone and ANEC saturation*, *JHEP* **05** (2023) 065 [arXiv:2210.16274] [INSPIRE].

[29] Y.-Z. Li, *Heavy-light bootstrap from Lorentzian inversion formula*, *JHEP* **07** (2020) 046 [arXiv:1910.06357] [INSPIRE].

[30] Y.-Z. Li and H.-Y. Zhang, *More on heavy-light bootstrap up to double-stress-tensor*, *JHEP* **10** (2020) 055 [arXiv:2004.04758] [INSPIRE].

[31] R. Karlsson, M. Kulaxizi, A. Parnachev and P. Tadić, *Stress tensor sector of conformal correlators operators in the Regge limit*, *JHEP* **07** (2020) 019 [arXiv:2002.12254] [INSPIRE].

[32] M. Dodelson and A. Zhiboedov, *Gravitational orbits, double-twist mirage, and many-body scars*, *JHEP* **12** (2022) 163 [arXiv:2204.09749] [INSPIRE].

[33] M. Dodelson et al., *Holographic thermal correlators from supersymmetric instantons*, *SciPost Phys.* **14** (2023) 116 [arXiv:2206.07720] [INSPIRE].

[34] M. Dodelson, C. Iossa, R. Karlsson and A. Zhiboedov, *A thermal product formula*, *JHEP* **01** (2024) 036 [arXiv:2304.12339] [INSPIRE].

[35] C. Esper et al., *Thermal stress tensor correlators near lightcone and holography*, *JHEP* **11** (2023) 107 [arXiv:2306.00787] [INSPIRE].

[36] E. Katz, S. Sachdev, E.S. Sørensen and W. Witczak-Krempa, *Conformal field theories at nonzero temperature: operator product expansions, Monte Carlo, and holography*, *Phys. Rev. B* **90** (2014) 245109 [arXiv:1409.3841] [INSPIRE].

[37] A. Manenti, *Thermal CFTs in momentum space*, *JHEP* **01** (2020) 009 [arXiv:1905.01355] [INSPIRE].

[38] M. Kulaxizi, G.S. Ng and A. Parnachev, *Subleading eikonal, AdS/CFT and double stress tensors*, *JHEP* **10** (2019) 107 [arXiv:1907.00867] [INSPIRE].

[39] R. Karlsson, M. Kulaxizi, A. Parnachev and P. Tadić, *Black holes and conformal Regge bootstrap*, *JHEP* **10** (2019) 046 [arXiv:1904.00060] [INSPIRE].

[40] R. Karlsson, *Multi-stress tensors and next-to-leading singularities in the Regge limit*, *JHEP* **08** (2020) 037 [arXiv:1912.01577] [INSPIRE].

[41] A. Parnachev and K. Sen, *Notes on AdS-Schwarzschild eikonal phase*, *JHEP* **03** (2021) 289 [arXiv:2011.06920] [INSPIRE].

[42] A. Parnachev, *Near lightcone thermal conformal correlators and holography*, *J. Phys. A* **54** (2021) 155401 [arXiv:2005.06877] [INSPIRE].

[43] R. Kubo, *Statistical mechanical theory of irreversible processes. 1. General theory and simple applications in magnetic and conduction problems*, *J. Phys. Soc. Jap.* **12** (1957) 570 [INSPIRE].

[44] P.C. Martin and J.S. Schwinger, *Theory of many particle systems. 1*, *Phys. Rev.* **115** (1959) 1342 [INSPIRE].

[45] A.L. Fitzpatrick, J. Kaplan, M.T. Walters and J. Wang, *Hawking from Catalan*, *JHEP* **05** (2016) 069 [arXiv:1510.00014] [INSPIRE].

JHEP10(2024)105

[46] G. Festuccia, *Black hole singularities in the framework of gauge/string duality*, Ph.D. thesis, http://hdl.handle.net/1721.1/45421, Massachusetts Institute of Technology, Cambridge, MA, U.S.A. (2007).

[47] L. Iliesiu et al., *The conformal bootstrap at finite temperature*, *JHEP* **10** (2018) 070 [arXiv:1802.10266] [INSPIRE].

[48] L.F. Alday, M. Kologlu and A. Zhiboedov, *Holographic correlators at finite temperature*, *JHEP* **06** (2021) 082 [arXiv:2009.10062] [INSPIRE].

[49] S. El-Showk and K. Papadodimas, *Emergent spacetime and holographic CFTs*, *JHEP* **10** (2012) 106 [arXiv:1101.4163] [INSPIRE].

[50] A.L. Fitzpatrick, J. Kaplan and M.T. Walters, *Universality of long-distance AdS physics from the CFT bootstrap*, *JHEP* **08** (2014) 145 [arXiv:1403.6829] [INSPIRE].

[51] Z. Komargodski and A. Zhiboedov, *Convexity and liberation at large spin*, *JHEP* **11** (2013) 140 [arXiv:1212.4103] [INSPIRE].

[52] E. Marchetto, A. Miscioscia and E. Pomoni, *Sum rules & Tauberian theorems at finite temperature*, *JHEP* **09** (2024) 044 [arXiv:2312.13030] [INSPIRE].

[53] S. Chapman et al., *Complex geodesics in de Sitter space*, *JHEP* **03** (2023) 006 [arXiv:2212.01398] [INSPIRE].

[54] L. Aalsma et al., *Late-time correlators and complex geodesics in de Sitter space*, *SciPost Phys.* **15** (2023) 031 [arXiv:2212.01394] [INSPIRE].

[55] A. Hamilton, D.N. Kabat, G. Lifschytz and D.A. Lowe, *Local bulk operators in AdS/CFT: a holographic description of the black hole interior*, *Phys. Rev. D* **75** (2007) 106001 [*Erratum ibid.* **75** (2007) 129902] [hep-th/0612053] [INSPIRE].

[56] A. Koshelev and A. Tokareva, *Non-perturbative quantum gravity denounces singular black holes*, arXiv:2404.07925 [INSPIRE].

[57] A. Frenkel, S.A. Hartnoll, J. Kruthoff and Z.D. Shi, *Holographic flows from CFT to the Kasner universe*, *JHEP* **08** (2020) 003 [arXiv:2004.01192] [INSPIRE].

[58] V.A. Belinsky, I.M. Khalatnikov and E.M. Lifshitz, *Oscillatory approach to a singular point in the relativistic cosmology*, *Adv. Phys.* **19** (1970) 525 [INSPIRE].

[59] C.W. Misner, *Mixmaster universe*, *Phys. Rev. Lett.* **22** (1969) 1071 [INSPIRE].

[60] M. De Clerck, S.A. Hartnoll and J.E. Santos, *Mixmaster chaos in an AdS black hole interior*, *JHEP* **07** (2024) 202 [arXiv:2312.11622] [INSPIRE].

[61] F.A. Dolan and H. Osborn, *Conformal four point functions and the operator product expansion*, *Nucl. Phys. B* **599** (2001) 459 [hep-th/0011040] [INSPIRE].

[62] F.A. Dolan and H. Osborn, *Conformal partial waves and the operator product expansion*, *Nucl. Phys. B* **678** (2004) 491 [hep-th/0309180] [INSPIRE].

[63] R. Karlsson, A. Parnachev and P. Tadić, *Thermalization in large-N CFTs*, *JHEP* **09** (2021) 205 [arXiv:2102.04953] [INSPIRE].

JHEP10(2024)105